UNIVERSITY OF CALIFORNIA
SANTA CRUZ

EVAPORATING WORMHOLES

A dissertation submitted in partial satisfaction of the
requirements for the degree of

DOCTOR OF PHILOSOPHY

in

ASTRONOMY & ASTROPHYSICS

by

Amita Kuttner

June 2019

The Dissertation of Amita Kuttner
is approved:

Professor Anthony Aguirre, Chair

Professor Enrico Ramirez-Ruiz

Professor Michael Dine

Lori Kletzer
Vice Provost and Dean of Graduate Studies

Table of Contents

List of Figures

Abstract

Evaporating Wormholes

by

Amita Kuttner

There has been a resurgence of interest in wormholes, and continued growth in the study of primordial black holes, opening up new questions about these objects and their possible existence in our universe. Recent papers demonstrate a new way of forming wormholes in the early universe, via collapsing inflationary bubbles. On our end, these wormholes would take the form of primordial black holes. This lends new interest to an intriguing and largely unaddressed question of what happens to a wormhole as the black hole on each end of it Hawking evaporates. Primordial wormholes would have an early period of traversability and we find, using calculations based on a semi-classical model of Hawking radiation, that as they evaporate they become traversable again to some degree. They then could evaporate to leave a Planck-size wormhole that may or may not persist. We also explore the implications of traversable wormholes and the questions that arise from their existence.

To my many parents...

who taught me to be.

Acknowledgments

I would not be doing what I am today, nor would I be who I am now were it not for my advisor, Anthony Aguirre. Thank you for the years of laughter and philosophy that punctuated our work in physics and now, also, improving the world.

I probably would not have been able to explain so much of what I worked on and have it be accurate without Joe Schindler, who also provided me with countless computed diagrams from his wonderful program. To the rest of our research group, Dominik and Ross, thank you for your insight over the years.

My deepest gratitude to everyone on my committees: Michael Dine, Howie Haber, Enrico Ramirez-Ruiz and Brant Robertson. Your help, time, and support and teaching have been essential. And of course without fellow students I would not have learned so well or lived. Nico, Andrew, everyone in my cohort, and all my now beloved friends I met at UCSC. Thank you to Katie for making everything possible by giving me a place to stay in my last year, and a lot more. Without friends for writing company, Stacey, and help editing, Eva, this writing process would have been a lot harder.

Technical tools whose developers saved me time deserve their moment, so to the creators of MathPix, Overleaf, and LaTeX, thank you!

To my large extended family, my mum who gave me life even though she left early, my dad, Babaji, Devaki, Melissa, my grandparents, and many more.

Music undeniably carried me through my degree, so thank you Cheryl and the Cabrillo Choruses for my voice. And thank you Lorchen for helping me get my mind and my freedom back. A most heartfelt thank you to the wonderful Larissa, whose continued friendship I cherish.

Many thanks to my campaign team, Keith, Max, Carrie, and my fearless leader Elizabeth for putting up with a candidate with other priorities (this thesis). I won't be able to list everyone, so to all who offered me support, you're wonderful and thank you.

Last but not least my dearest companions made it possible for me to do this work; Amoosh, Pancakes, Aspen, and Alpine, you're all the best. My husband Ian did far too much to give me the time to do so much at once, I love you.

I am grateful for the time I have been given on this Earth, and I hope to do good by it.

The text of this dissertation includes, with permission, partial reprints from the following soon to be published material (in preparation, title may change): J. Schindler, A. Aguirre, A. Kuttner, "Visualizing black hole evaporation with explicitly computed Penrose diagrams" (2019) [65].

Chapter 1

Introduction

Einstein's theory of General Relativity leaves many open doors, and many open questions. The theory itself is beautifully complete but for the looming mystery of quantum gravity. When it comes to applications of General Relativity, there are a host of spacetimes that are solutions to Einstein's equations where it is unknown whether or not they are physical, i.e. possible in our universe. Long relegated to solutions of purely mathematical interest, *wormholes* have lately found a resurgence of interest. And at the intersection of the quantum gravity wilderness and well-used spacetime solutions, lies the central topic of this dissertation: the nature of evaporating wormholes.

1.1 Black Hole Evaporation

When Stephen Hawking introduced the concept of black hole (hereafter abbreviated as BH) evaporation in 1974, it came as a surprise [36]. The idea that BHs have a thermal signature seemed contrary to their definition. Since Hawking's original paper, a great deal of work has been done [57], with much controversy [71]. And there are a number of key open questions that remain, many of which relate to this thesis.

For instance, we are still wondering if the entire process of BH evaporation is unitary, meaning that information would be preserved. Hawking's original paper suggested that information would not be preserved, but he famously changed his mind later [39]. And if information is preserved, we would like to know how the initial state is then encoded in emissions from the BH. The current consensus is that BH evaporation is unitary, but there is no consensus answer to how the information is preserved [61, 54].

Second, Hawking radiation reveals BHs to be bona fide thermodynamic objects, which should be accorded entropy. Bekenstein's and others' pioneering work has offered a widely-accepted quantification of BH entropy [10], calculated as a quarter of the surface area (in Planck areas); but this does not tell us what the *nature* of the entropy is, or what exactly this quantity is counting. Moreover, we still do not know how the thermodynamics of evaporation should be

understood. The "generalized second law," for example, indicates that entropy should increase throughout evaporation, but includes multiple types of entropy with fundamentally different definitions [11].

Third, if information is destroyed in a BH, it would be problematic because it would turn a pure quantum state into a mixed state. One treatment of this problem has resulted is the idea of BH Complementarity, suggested by Susskind and et al. in 1993 [72], which says that information is both reflected on the horizon *and* passes through it, depending on which observer you ask; and the area just above the horizon acts just like a membrane that scrambles the information and re-emits it as Hawking radiation, preserving unitarity. The famous "firewall" elaboration to the BH information paradox, developed by Almheiri et al. [4], arose from a suggestion about how to solve the fundamental inconsistencies between Einstein's equivalence principle, laws of quantum theory, and local field theory, and as a response to the idea of complementarity. One resolution to this apparent inconsistency is to let go of the equivalence principles, allowing for a region of Planck-level energy density at the horizon that would destroy infalling things.

There has been little clarity on what exactly the spacetime structure of evaporating BHs is supposed to be like or to look like. Ostensibly, there should be an ideal way to consider it that takes into account the fact that the *event horizon*, often taken as the defining characteristic of a BH, does not really exist as such in

an evaporating BH, and should be replaced with an apparent horizon [65]. The original structure suggested in diagrammatic form by Hawking is problematic, which Hawking himself, as well as others, have pointed out, offering suggestions for more accurate pictures [39, 41].

These open issues cover most of what is still highly debated about BH evaporation. Due to how contentious this subject is, we have tried to bring some clarity to the spacetime structure of evaporating BHs by developing a model of Hawking radiation that can be explicitly computed in algorithmically-generated Penrose diagrams. This work informed but is not presented in this thesis as it is not the intended purview [65]. During the course of that work, we came upon the suggestion that extended Schwarzschild wormholes could exist in our universe. This encouraged us to consider what would happen if those wormholes evaporate.

1.2 Wormhole Evaporation

Wormholes are objects that connect two large regions of spacetime via a narrow "throat," and may have a BH on either side. Wormhole evaporation has been investigated relatively little, presumably because the existence of wormholes is questionable – unlike the approximate certainty that BHs enjoy. At the time of this writing, there has been relatively little explicit discussion of evaporating wormholes compared to evaporating BHs, though there is more and more conversation

around the existence of wormholes and wormhole behavior [5, 13, 63, 9, 33, 44, 68].

We should begin by clarifying (with more discussion to come later) that there are two commonly-discussed types of wormhole: time-independent *traversable* wormholes (the "Ellis" wormhole discussed below being a prime example), and the extended Schwarzschild metric or Einstein-Rosen Bridge ("ER bridge"). These spacetime forms are related: for example the ER bridge can be converted into a traversable wormhole [40, 43, 49, 67], or vice-versa, via the addition of negative or positive energy or matter respectively.

The relative paucity of study of wormholes relative to black holes stems from their rather more speculative nature. As we will explain, a traversable wormhole requires exotic matter or energy that violates energy conditions. And the extended Schwarzschild solution is mathematically well known, but has remained a theoretical extension of the metric used to describe BHs formed from collapsed stars. In those descriptions, most of the extended spacetime is gone because the relevant exterior portion has been matched onto the collapsing and collapsed star as an interior solution. Since the exterior of the BH is connected to a collapsing object (and therefore does not include the rest of what the mathematics describes would exist in the metric), what we understand to be a BH is only a portion of Schwarzschild connected to a collapsed object. Though it is well studied, there has been no known good way to *produce* ER bridge spacetimes (by which we mean there is no know way they would have come into existence). Similarly, with Ellis

wormholes, there is no known process by which to produce the exotic matter necessary to sustain them, and moreover the very absence of such matter constitutes a very widely assumed set of conditions in classical relativity.

Yet if physically existent, ER bridges (or "Schwarzschild wormholes") should, arguably, evaporate, because the spacetime "outside" a Schwarzschild wormhole is identical to that outside a Schwarzschild BH, and has no way of knowing if what exists is just a BH or a wormhole, the presence or absence of which is only ostensibly noticeable past the horizon. Therefore the Quantum Field Theory (QFT) calculations describing BH evaporation should apply to both sides of the wormhole, and there should be the same flux on each side of the wormhole as with a Schwarzschild BH.

Moreover, there is now a compelling proposal by Garriga et al. and Deng et al.[32, 24] for how wormholes of the ER Bridge type can form during the inflationary epoch of the early universe, through the collapse of inflationary bubbles whose interiors continue to inflate. This scenario is much less speculative than previous considerations of wormholes, and might even be amenable to observational and experimental investigation. The papers cited above include simulations and expected mass spectra for these black/worm holes.

1.3 Our Goals

The aim of this thesis is to explore questions about the causal structure of an evaporating ER Bridge wormhole. Such a scenario could possibly exist as a result of the early-universe inflationary bubble collapse mentioned above. Whether or not the ER Bridge wormholes we evaporate are tied to such a formation scenario, it is independently interesting to see how they work.

In order to model the evaporation process, we will use a method similar to that presented by J. Schindler, A. Aguirre, and A. Kuttner (hereafter written as SAK) [65] with null shells standing in for Hawking radiation; evolving spacetime solutions are created by piecewise assembly of time-independent solutions, with junctions between those solutions enforcing Einstein's equations at the boundaries and the conservation of stress-energy.

We assume that both sides of the wormhole evaporate, and we investigate the implications of evaporation. We will discuss in detail two fascinating possibilities that arise from our evaporation calculations. First, we find that evaporation renders ER bridges traversable; second, we provide a suggestion as to what could happen at the end of evaporation.[1]

[1]Late in this work we discovered work by Hayward using the Vaidya spacetime which showed an ER Bridge becoming a traversable Ellis wormhole [43, 49]; this is related to - but differently motivated and somewhat distinct from - the evaporation process we describe.

Chapter 2

Static Black and Worm Holes

In this chapter, we will review the definitions of static BHs and wormholes, as well as the theorems that govern them. We also discuss the visualization of spacetimes using conformal diagrams, BHs with regularized interiors, and energy conditions.

2.1 Black Holes

2.1.1 Schwarzschild Metric

The Schwarzschild metric is the metric used to describe the simplest of BHs. It is actually quite general, as it is the unique spherically-symmetric vacuum metric and thus the metric for the spacetime around any spherical, gravitating body as long as it is not significantly charged or rotating. It was found by Schwarzschild

in 1916 [66] and has line element

$$ds^2 = -\left(1 - \frac{2M}{r}\right)dt^2 + \left(1 - \frac{2M}{r}\right)^{-1} dr^2 + r^2 d\Omega^2 \tag{2.1}$$

in spherical spacetime coordinates, where M is the mass of the gravitating body, and $d\Omega$ is line element of a unit sphere. We are working with the metric signature $(-1, 1, 1, 1)$ and with constants $G = c = 1$.

This metric has a couple of interesting and important features, namely that it is undefined and goes to infinity at $r = 0$ and $r = 2M$. For objects like stars and planets this does not really matter because the undefined radii are inside the body of the object, where the Schwarzschild metric would not be appropriate to describe the spacetime. The Schwarzschild metric can apply here when the $r = 2M$ sphere could exist outside the object (making it a BH), in which case the Schwarzschild metric can apply all the way to $r = 0$, which is then a gravitational singularity. As the metric describes a vacuum solution, if it holds everywhere then no mass exists in the spacetime – all of the mass is defined to be at the $r = 0$ singularity.

The Schwarzschild radius is defined, with constants, as $r_s \equiv \frac{2GM}{c^2}$. Unlike $r = 0$, it comprises a coordinate singularity, meaning that there is no local physical divergence or discontinuity there. When the metric is translated into other coordinate systems (that by nature define the same curvature and spacetime), nothing observable exists there, and there is no longer a discontinuity. This means an ob-

server moving across the Schwarzschild radius would not notice anything. [1] In a static BH, r_s is the radius which defines the event horizon, the point of no return, which is characterized by surfaces of constant radius changing from being time-like to being spacelike (and thus like "times"). An observer inward of the event horizon moving forward in proper time has no choice, while moving within their lightcone, but to move to smaller radii and eventually the singularity.

2.1.2 Conformal Diagram

In order to visualize the Schwarzschild metric and others, we need to plot them in a sensible way. We need a spacetime diagram that uses conformal mapping to preserve the lightcones (chosen to be 45 degree angles) and fit the entire spacetime and its infinities into a finite diagram. Such diagrams are known as Penrose-Carter diagrams, or conformal diagrams. The first step is to put the Schwarzschild metric into coordinates that are well-behaved across the entire spacetime. Definitions and descriptions in this section are drawn from Hawking and Ellis, and Carroll [37, 17].

The Kruskal-Szekeres metric is a re-coordinatization of the Schwarzschild metric that does not have any coordinate singularities, and is well-defined everywhere outside $r = 0$ [51]. The Kruskal-Szekeres coordinates transform the

[1] By the classical understanding of Schwarzschild, nothing would be noticeable across the horizon; but if there is indeed a firewall there, one would encounter it.

Schwarzschild t, r into u, v

$$\begin{aligned} u &= \left(1 - \frac{r}{2M}\right)^{1/2} e^{r/4M} \cosh\left(\frac{t}{4M}\right) \\ v &= \left(1 - \frac{r}{2M}\right)^{1/2} e^{r/4M} \sinh\left(\frac{t}{4M}\right) \end{aligned} \tag{2.2}$$

turning the metric into

$$ds^2 = \frac{32M^3}{r} e^{-r/2M} \left(-\mathrm{d}v^2 + \mathrm{d}u^2\right) + r^2 d\Omega^2, \tag{2.3}$$

where r is now defined implicitly via

$$\left(u^2 - v^2\right) = \left(\frac{r}{2M} - 1\right) e^{r/2M}. \tag{2.4}$$

This form plotted results in very warped angles; to help fit them into a finite size, the Kruskal-Szekeres coordinates should be changed into their null version with

$$\begin{aligned} u' &= u - v, \\ v' &= u + v \end{aligned} \tag{2.5}$$

so that the metric reads

$$ds^2 = -\frac{16M^3}{r} e^{-r/2M} \left(\mathrm{d}u'\mathrm{d}v' + \mathrm{d}v'\mathrm{d}u'\right) + r^2 d\Omega^2 \tag{2.6}$$

where r is now

$$u'v' = \left(\frac{r}{2M} - 1\right) e^{r/2M}. \tag{2.7}$$

The last step is one more transformation to make a good looking Penrose diagram, stretching the infinities into the corners. We now define coordinates

$$\begin{aligned} U &= \arctan\left(\frac{u'}{\sqrt{2M}}\right) \\ V &= \arctan\left(\frac{v'}{\sqrt{2M}}\right) \end{aligned} \tag{2.8}$$

which have the ranges

$$\begin{aligned} -\pi/2 < U < +\pi/2 \\ -\pi/2 < V < +\pi/2 \\ -\pi < U + V < \pi \end{aligned} \tag{2.9}$$

and can now be plotted into diamond edged spacetime diagrams, with lines of constant r and t plottable over top. This is because it is now conformal to Minkowski, and Schwarzschild has two infinite regions that are like Minkowski at large r. The coordinates U, V are orthogonal and sit at 45 degrees from vertical. In this diagram every point is a two sphere, as the spherical symmetry is compressed, leaving only the time axis and one spatial axis. With these transformations and this diagram, we now have a tool with which to envision and understand the spacetime.

Penrose diagrams are labeled with the following notation

$$\begin{aligned} i^+ &= \text{ future timelike infinity} \\ i^0 &= \text{ spatial infinity} \\ i^- &= \text{ past timelike infinity} \\ \mathcal{I}^+ &= \text{ future null infinity} \\ \mathcal{I}^- &= \text{ past null infinity} \end{aligned}$$

which helps identify where on the diagrams different infinities have been encoded. For example, figure 2.1 shows a Penrose diagram for an eternal Schwarzschild BH formed from stellar collapse or similar.

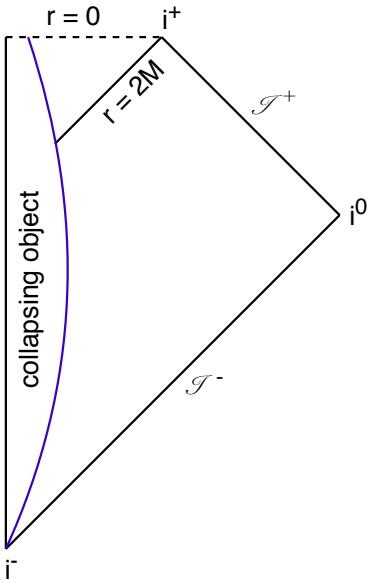

Figure 2.1: Cartoon Penrose diagram of Schwarzschild formed by the collapse of an object, or region of matter. Infinities are as marked, the dashed line represents the gravitational singularity at $r = 0$, the purple line the edge of the collapsing matter, and the horizon is noted at $r = 2M$. The vertical edge on the left side is also $r = 0$, the center of the collapsing object.

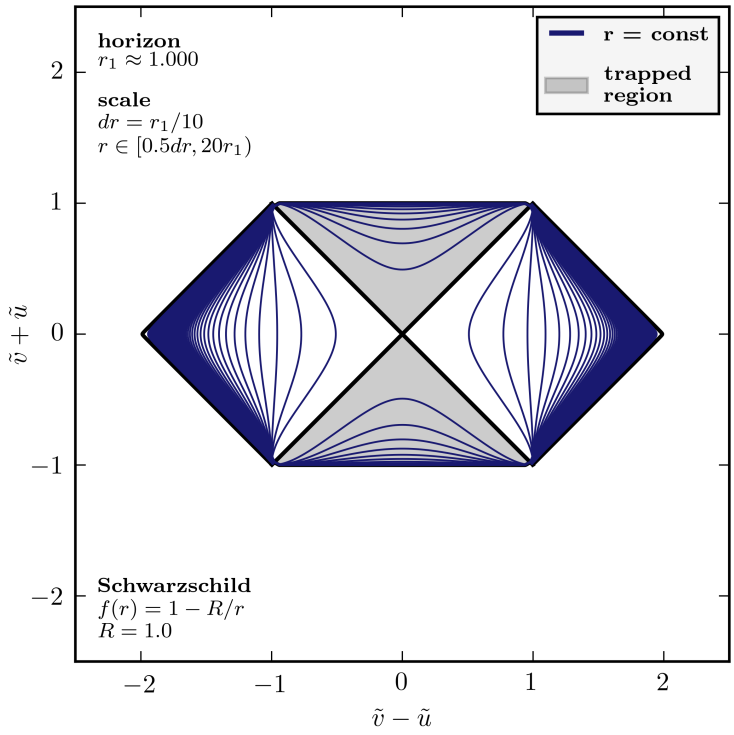

Figure 2.2: Computer plotted Penrose diagram for the extended Schwarzschild metric, with lines of constant r. Source: J. Schindler

2.1.3 Defining a Black Hole

The term "black hole" comes from the concept that nothing can propagate acausally, and thus nothing inside the horizon can be seen outside of it. Wald's definition states that a BH is a "region of no escape" that does not extend to infinity [76]. (We question whether this is an accurate or sufficient definition given recent BH discussions and propose a more nuanced idea in our paper; see SAK for this analysis [65].) Such an object is formed when a large enough mass is enclosed in a corresponding radius. This can occur, for example, when an object has large enough mass that it can no longer maintain hydrostatic equilibrium. Singularity theorems and the black hole "no hair theorem" discussed below then point to an end-state described by a stationary BH spacetime [76].

The fact that the gravitational singularity is hidden from view is encapsulated in the cosmic censorship conjecture, which states that gravitational collapse will never produce a naked singularity, i.e. if a singularity is formed it will always be hidden behind a BH horizon.

Black Holes may also have other properties, such as angular momentum and charge, and therefore may have electromagnetic fields. Ostensibly, there could exist many different variations of BHs and BH metrics; but regardless of its properties during formation, a BH will simplify by giving off gravitational radiation and settle to a state in which it can be defined only by mass, charge, and angular

momentum [17]. This is known as the "no-hair" theorem. The Kerr-Newman metric covers all other types, having angular momentum and charge, and turns into the Schwarzschild when both vanish. The Kerr metric is rotating only, and the Reissner-Nordstrom metric is charged only. Other metrics may add to the spacetime, such as the Schwarzschild-de Sitter metric; but in this metric the BH is very similar to a Schwarzschild BH, with its horizon changed due to the de Sitter vacuum, as it is a metric with a non-zero cosmological constant.

2.1.4 The Einstein-Rosen Bridge

As one can see from plotting the Schwarzschild metric in a conformal diagram, there is more in the mathematics than an object collapsed into a BH. The maximally extended Schwarzschild metric has two "universes" (regions of very large or infinite nearly-flat space) connected by a white hole and a BH. Figure 2.2 shows the Penrose diagram for the extended Schwarzschild solution. The region past the BH horizon is accessible from both universes, but the wormhole is not traversable because if anything falls in, it cannot causally get back out; conversely nothing can get *in* to the white hole (it can only be in an observers past, not their future).

The extended Schwarzschild metric and the Schwarzschild metric introduced above (used to describe collapsed spherical bodies) do not differ mathematically, but represent different things. The region of the Schwarzschild metric that is used in the diagram of collapsed bodies is assumed to be connected, or "junc-

tioned," onto the collapsed star (or other collapsed material) metric, along the boundary of the outer edge of the object, and thus part of the full Schwarzschild spacetime is absent. We will describe how metrics are mathematically junctioned in a later section. Up until recent papers [32, 24] it seemed that there was no way for the extended Schwarzschild to represent anything that could actually be formed in our universe, and that it was thus an unphysical and purely theoretical extension, even if it has been explicated and studied extensively. Further discussion of the meaning of the extended Schwarzschild metric is now needed. We will touch on it after the introduction of the primordial wormhole (whose junctioned metrics and diagram incorporate the extended Schwarzschild).

This vacuum solution is one example that is said to contain an Einstein-Rosen (ER) bridge, after the paper by Einstein and Rosen that discussed the connection between two universes that is apparent in extended Schwarzschild [27]. An ER bridge is characterized by two separate spatial regions with their own infinities. There has also been discussion about possible entanglement at the cross point in the middle between the two universes [53]. This is considered a wormhole, but it is not traversable as it stands because the only connection between the two universes – the BH – will not let you out again. The existence of an ER bridge does not violate any energy conditions, though is it possible there are other reasons it could be unphysical.

2.1.5 Regularized Interior

The singularity inside a BH is not necessary for its definition, though it is tied to the existence of "trapped surfaces" (which are in turn connected to horizons) by the Hawking-Penrose black hole singularity theorems [76]. However, these theorems assume the Strong Energy Condition. If energy conditions are relaxed, possibilities exist for *non*singular BHs with a very similar structure to the Schwarzschild solutions.

The metric for a BH with a regularized (non-singular) interior presented by Hayward has been useful to us in our BH evaporation methodology. It is essentially composed of a Schwarzschild exterior and a de Sitter interior, with the line element

$$ds^2 = -\left(1 - \frac{2mr^2}{r^3 + 2l^2m}\right)dt^2 + \left(1 - \frac{2mr^2}{r^3 + 2l^2m}\right)^{-1} dr^2 + r^2 d\Omega^2, \qquad (2.10)$$

where we have coordinates as before, and positive constants m, l. Here m is the mass parameter, and l is connected to the scale of the de Sitter region. We will generally take the latter to be at the Planck scale, which governs the density and curvature cut-off for quantum effects in the core. As can be seen in figure 2.3, which is the cartoon conformal diagram given by Hayward, this non-singular metric has an inner and an outer horizon. The outer horizon is the event horizon we know well from Schwarzschild, and the inner horizon is the de Sitter horizon. The metric has no gravitational singularity at $r = 0$, and its outer horizons arise

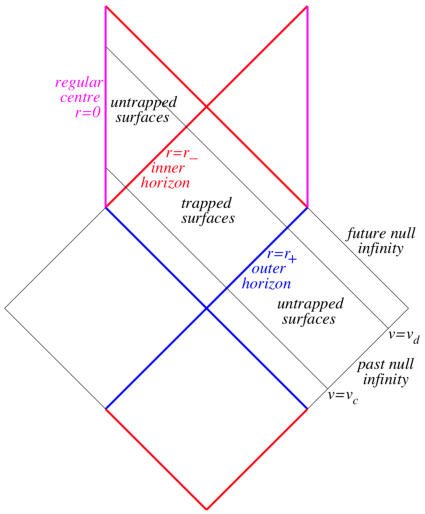

Figure 2.3: Illustrated conformal diagram for a Hayward black hole. Source: Hayward [41].

from the same mechanism as in Schwarzschild.

We used the Hayward metric because we wanted to create a classically analyzable metric that is a stand-in for a metric that becomes non-classical due to quantum gravity effects as the curvature scale become Planckian. So this metric, which has density in the core, provides a semi-classical analog for the region dominated by quantum gravity effects within a BH.

Notably, this metric, which we shall refer to as the Hayward metric, still has an ER bridge and therefore has the relevant properties described above of two universes connected by a non-traversable BH. This metric is one of the basic components of the BH evaporation calculations presented in SAK [65]. It proved useful in evaporating a BH as there was a desire to approach it in a way that avoided having a singularity to contend with at the end of evaporation. It is

also useful, but not necessary, in the matching needed in the evaporation of a wormhole.

2.2 Wormholes

2.2.1 Defining a Wormhole

Wormholes are theoretical spacetime objects, mathematically described by spacetime metrics. The basic concept is that a wormhole is a connection between two areas of spacetime that would not otherwise be accessible to each other. Their existence in our universe is questionable because traversable wormhole solutions violate energy conditions (we will cover the relevant condition later).

The general idea of a wormhole can be seen in a spherically-symmetric spacetime, in which surfaces of constant time and radius r are two-spheres. Suppose that as $r \to 0$, the size of a sphere decreases and goes to a minimum, then starts getting bigger again. Then this region of small r exists as a connection between two separate spaces or universes where r gets very or unboundedly large. Wormholes were named as such because of constant-time hypersurfaces looking like tunnels that worms make, but if we were to observe a wormhole it would not look like a tube – we would be confined to the "walls" of the tube and would simply see photons from the other side distorted by the geometry through which they propagate.

There are two basic wormholes to consider for our purposes here: the extended Schwarzschild ER bridge, described above, and the "Ellis wormhole." They have many properties that differ from each other. The Ellis metric is just a wormhole (curvature to a minimum r and back out), whereas the ER bridge has a connection to an area that has a separate $r = 0$. The Ellis metric describes a wormhole between separate spatial regions, but this could be a portion of a larger picture; sometimes it is imagined that the large joined regions are actually the same region. With the extended Schwarzschild metric, one also has to contend with a white hole, which the Ellis metric does not contain.

2.2.2 Ellis Metric

The Ellis wormhole, also called a Morris-Thorne wormhole due its separate introduction as a teaching tool in 1988 by Morris and Thorne [55], is the most basic description of a wormhole. The Ellis wormhole metric has the line element

$$ds^2 = -dt^2 + dr^2 + (r^2 + n^2)d\Omega^2, \tag{2.11}$$

where n is "neck," the length scale of the "funnel," and the other variables are spherical spacetime coordinates. The conformal diagram for the Ellis wormhole is shown in figure 2.4. It resembles flat space, the conformal diagram for the Minkowski metric, and is asymptotically flat. In particular it resembles a flat universe on each side and going towards $r = 0$ in the center. It differs by not being

a vacuum solution, and only getting down to $r = n$. In Minkowski, there is no matter or energy creating curvature; in Schwarzschild, the curvature is generated by the mass at the gravitational singularity, therefore allowing the spacetime to be vacuum. The curvature in Ellis is generated in the spacetime at the neck, which has nonzero energy-momentum tensor.

The energy-momentum tensor $T_{\alpha\beta}$ of the Ellis metric violates the Weak Energy Condition (WEC)

$$\rho = T_{\alpha\beta} X^{\alpha} X^{\beta} \geq 0 \tag{2.12}$$

which states that for any timelike vector field X, the matter density, ρ as observed in the rest frame defined by that vector field must be non-negative. The Ellis metric has

$$\rho = -\frac{1}{n^2(1 + (\frac{r}{n})^2)^2} \tag{2.13}$$

for

$$X = \frac{1}{(1 + (\frac{r}{n})^2)^2}, \tag{2.14}$$

which is negative and therefore violates the WEC. The density ρ goes to zero far away from the wormhole throat, and is larger for a smaller throat.

The energy conditions exist to limit solutions to Einsteins equations since not all solutions that are possible are necessarily physical. Satisfying energy conditions is supposed to ensure that the energy and matter conform to particular fundamental restrictions. The Strong Energy Condition, for example, ensures

that gravity is attractive; the above Weak condition requires energy to be positive. Others disallow faster-than-light energy transfer and other effects. These are crucial because it is important to determine if mathematically-defined spacetime metrics are physical as that is how we can relate them to our astrophysical world.

It is important to note, however, that it is quite possible on a *quantum* scale to violate any and all of these energy conditions.

The Ellis wormhole, if it could exist, and if the exotic matter itself would not prove an impediment, would be *traversable*, meaning non-spacelike paths can go from one side of the wormhole to the other; this is manifest in the conformal diagram. One should also note that in this metric on the conformal diagram, points are still 2-spheres, but no longer of radius r (but rather $(r^2 + n^2)^{1/2}$).

While the Ellis wormhole is a special case, traversability will arguably *generally* violate energy conditions because it requires a geodesic congruence where they change from outward to inward or vice-versa, a hallmark of violations of the *Null* energy condition [17].

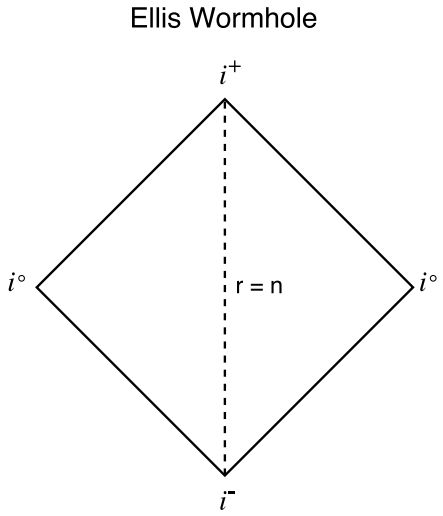

Figure 2.4: Penrose diagram for an Ellis wormhole. Each side resembles Minkowski going out to infinity, but at the center it never reaches 0. The dashed line represents the minimum radius of the neck $r = n$.

Chapter 3

Matching Metrics

3.1 Motivation

Many physical situations of interest require solutions to Einstein's equations that are not among the relatively small catalog of known exact analytic solutions. It is therefore often useful to combine solutions by matching them onto each other at specified boundaries in order to create composite solutions capable of describing a range of situations. In cases we will look at, symmetries allow for an exact solution in several regions, which can be joined across a localized sheet or bubble of mass or energy.

Multiple formalisms exist for matching metrics (depending on the hypersurface along which the matching is done) to ensure that the composite solution is still a solution to Einstein's equations and does not violate any fundamental

laws. Einstein's equations then generally transform into equations constraining or governing the mass/energy joining the solutions.

In this section, we review the general process of matching across a *null* surface, describe the constraints that energy-momentum conservation places on the spacetime matching, and give a sketch of matching across a timelike surface.

3.2 Mathematics

The mathematical idea of matching is to ensure that the junction solves Einstein's equations, so that they are solved across the entire matched spacetime. The matching must be continuous, with a (Dirac) δ function source between the domains. In other words, we match regions with different structure for the energy-momentum tensor, where the energy-momentum tensor change is modeled as a θ-function and/or δ-function, and the metric is required to be continuous at the boundary. We look at the matching hypersurface, Σ, which is a submanifold of the spacetime manifold, and can be spacelike, timelike, or null. The hypersurface is defined by a function that restricts a coordinate to only one value.

The process begins by using appropriate coordinates on the hypersurface and defining the induced, or intrinsic, metric for it, and ensuring its continuity. Depending on which type of matching one is interested in, one would continue by determining the matter content of the shell, checking for conservation of energy,

and making sure the coordinates actually can match to each other at the surface (for instance with radii at a null match).

The overview of matching methodology given in this chapter is based on a number of sources. Though they were not the first, the traditional references for junctioning metrics are Israel [45], and Barrabès and Israel [7]; we also found the formulations by Poisson [60, 59] and Padmanabhan [56] very helpful, as well as the overview presented by Schindler [64]. The relation used to ensure energy conservation across matched shells was introduced by Dray and 't Hooft [26] and Redmount [62].

3.2.1 Null Match

The general formalism as laid out by Poisson [60] begins with the definition of intrinsic coordinates and tangent vectors to the hypersurface Σ. We will give a significantly summarized version here. Coordinates on Σ are defined as

$$y^a = \left(\lambda, \theta^A\right), \tag{3.1}$$

where index a runs over $1, 2, 3$, and index A runs over $2, 3$. So we have $y^1 = \lambda, y^2 = \theta^2$, and $y^3 = \theta^3$. These coordinates, y^a, are the same on both sides of the hypersurface. They are parametrized from the coordinates in the external metrics by $x^\alpha = x^\alpha\left(y^a\right)$, so we can define tangent vectors as $e^\alpha_a = \frac{\partial x^\alpha}{\partial y^a}$. Given the above

definition of the intrinsic coordinates we have null vectors

$$k^\alpha = \left(\frac{\partial x^\alpha}{\partial \lambda}\right)_{\theta^A} \equiv e^\alpha_\lambda \tag{3.2}$$

and spacelike vectors

$$e^\alpha_A = \left(\frac{\partial x^\alpha}{\partial \theta^A}\right)_\lambda \tag{3.3}$$

of which there are sets for each side of the hypersurface. The only non-zero inner products give us the induced metric on Σ

$$\sigma_{AB}\left(\lambda, \theta^C\right) \equiv g_{\alpha\beta} e^\alpha_A e^\beta_B, \tag{3.4}$$

that is required to be the same on both sides, which we write as

$$[\sigma_{AB}] = 0 \tag{3.5}$$

where the brackets are notation to indicate the difference across the hypersurface, having the form $[A] = A^+ - A^-$, with the + and − indicating the two sides of Σ.

We must also look at null transverse vectors (null normals), $N^\alpha_\pm$, defined as

$$N_\alpha N^\alpha = 0, \quad N_\alpha k^\alpha = -1, \quad N_\alpha e^\alpha_A = 0. \tag{3.6}$$

There is also the requirement that the congruence of timelike geodesics at the hypersurface is smooth. Along a single geodesic, we have $dx^\alpha_\pm = u^\alpha_\pm d\tau$, with proper time τ. For the congruence of geodesics to be smooth, $u^\alpha_\pm$ has to be the same. This can be written

$$[-u_\alpha k^\alpha] = 0 = [u_\alpha e^\alpha_A]\,. \tag{3.7}$$

This is required for the matching, but it is not essential in calculations to determine the hypersurface matter content. We have everything we need to find the transverse curvature and the energy momentum tensor of the shell. The transverse curvature is the curvature given to the hypersurface, as it is defined by the curvature of the spacetimes on either side of it using the normal vectors and coordinate parametrization. The transverse curvature of the shell is given by

$$C_{ab} = -N_\alpha e^\alpha_{a;\beta} e^\beta_b = C_{ba}. \tag{3.8}$$

Likely it is discontinuous, and said discontinuity will give us the information we need to define the content of the shell. We can define μ, j, p by these discontinuities in the transverse curvature, and using the intrinsic metric we have

$$\begin{aligned} \mu &= -\frac{1}{8\pi}\sigma^{AB}\left[C_{AB}\right] \\ j^A &= \frac{1}{8\pi}\sigma^{AB}\left[C_{\lambda B}\right] \quad , \\ p &= -\frac{1}{8\pi}\left[C_{\lambda\lambda}\right] \end{aligned} \tag{3.9}$$

and therefore the surface energy-momentum tensor can be written,

$$S^{\alpha\beta} = \mu k^\alpha k^\beta + j^A\left(k^\alpha e^\beta_A + e^\alpha_A k^\beta\right) + p\sigma^{AB} e^\alpha_A e^\beta_B. \tag{3.10}$$

The complete energy-momentum tensor is given by

$$T^{\alpha\beta}_\Sigma = \left(-k_\mu u^\mu\right)^{-1} S^{\alpha\beta}\delta(\tau). \tag{3.11}$$

It is important to understand the details of this formalism, but we were able to use a simplified version because we primarily worked with strongly spher-

ically symmetric (SSS) spacetimes. Such spacetimes are defined by Schindler [64] as being capable of having their line element in the form

$$ds^2 = -f(r)dt^2 + f(r)^{-1}dr^2 + r^2 d\Omega^2 \tag{3.12}$$

with a function $f(r)$. There are further properties to SSS spacetimes, which are discussed in that paper. Here a radial null hypersurface will result in the induced metric line element

$$ds^2 = r^2 d\Omega^2 \tag{3.13}$$

where the coordinates are parametrized as in the above formalism $x^i = (r, \Omega)$. Joining metrics like this requires that the radii match across Σ, which can be done algorithmically across multiple boundaries. Here we will use a simplification to Eddington-Finkelstein coordinates, which together with the induced metric above, through the formalism, yields an easy to use definition of the energy-momentum tensor

$$T^{ab}_{\Sigma} = \sigma n^a n^b \delta(w) \tag{3.14}$$

where

$$\sigma = (-\epsilon)\frac{[m(r)]}{4\pi r^2}, \tag{3.15}$$

and $n^a = \epsilon\,(\partial_r)^a$ and $\epsilon = \pm$ indicates an outgoing, $+$, or ingoing, $-$, shell and δ is the Dirac δ-distribution (w being the constant null coordinate on which the hypersurface is defined). For a more detailed exposition of how this simplified set

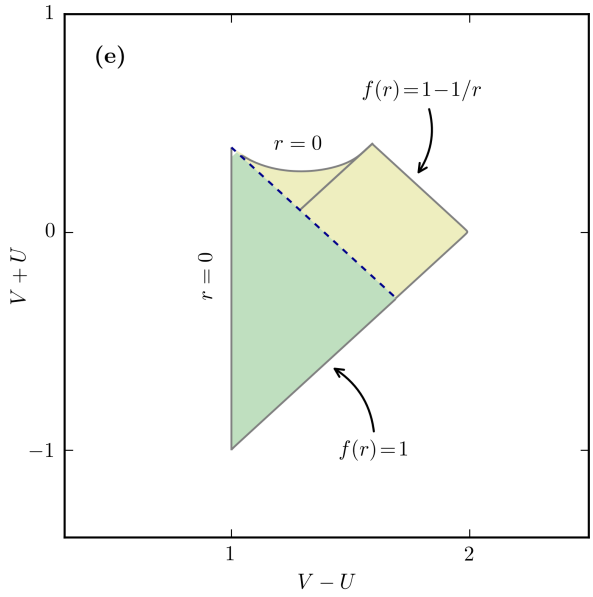

Figure 3.1: A computed diagram of matching Minkowski to Schwarzschild, which is created by an incoming shell of matter at the dashed line. The axes list the U, V coordinates from the Penrose diagram generation procedure. Source: J. Schindler.

of equations reduces from the null shell formalism above, see Schindler [64]. Here, $[m(r)]$ is defined via

$$[m(r)] = m_+(r) - m_-(r) \tag{3.16}$$

where $m(r)$ is a mass parameter that has been defined by placing the function $f(r)$ in the form

$$f(r) = 1 - \frac{2m(r)}{r}. \tag{3.17}$$

In figures 3.1 and 3.2 we see the algorithmically generated diagrams for the matching of Minkowski (in green) to Schwarzschild (in yellow) created via an incoming shell of matter.

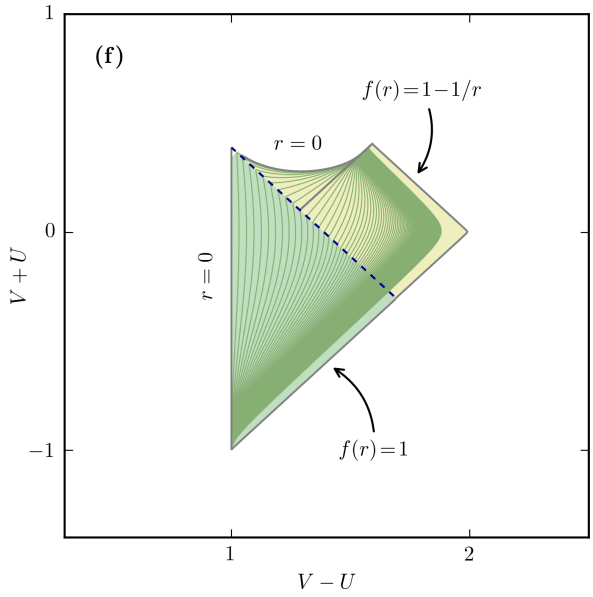

Figure 3.2: This is a computed diagram of the same match of Minkowski and Schwarzschild that also shows lines of constant r which have been matched across the hypersurface. Source: J. Schindler.

3.2.2 Energy Conservation

It is important to make sure matched metric spacetimes conserve energy. Shell junctions, matches between two metrics across one boundary, by construction conserve energy [7]; but this is not as immediately clear at corner junctions, where there are two thin shells crossing. The layout of these junctions can be seen in figure 3.3. For corner junctions we use the DTR relation

$$f_A(r_0)\, f_B(r_0) = f_C(r_0)\, f_D(r_0) \tag{3.18}$$

with the spacetime regions defined in figure (3.3). This relation is named for Dray, 't Hooft, and Redmount [26], [62]. This relationship encapsulates conservation of

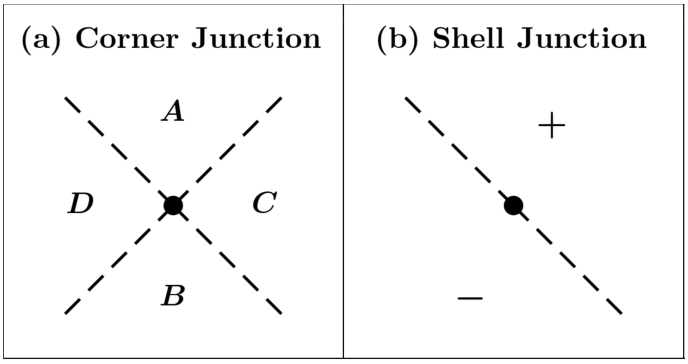

Figure 3.3: These are the two types of junctions we will consider: (a) corner and (b) shell. Source: J. Schindler [64].

energy at a junction between four regions. It is derived by looking at the four shells that meet, relating them to each other, and restricting the parameters to ensure conservation of mass and gravitational energy. As per the summary provided by Schindler [64], the DTR relation is necessary to show conservation of energy and probably is also sufficient.

The DTR relation may be used for slightly more generalized spacetimes as well. For these we look at metrics that can be written with line elements defined by

$$ds^2 = -e^{-2\phi(r)} f(r) dt^2 + f(r)^{-1} dr^2 + r^2 d\Omega^2, \tag{3.19}$$

which differ from the SSS spacetimes by the exponential of ϕ, which like $f(r)$, is a real function.

3.2.3 Timelike and Spacelike Matching

It is also possible to match across timelike and spacelike surfaces. It is actually a slightly simpler formalism than the null matching. We will not go over it in as much detail because we do not use it explicitly in the work presented here. Still, it is necessary to understand the research that inspired our work – the papers by Garriga, Vilenkin, Zhang, and Deng [32], [24] about BHs formed in the early universe.

Matching across a spacelike or timelike surface requires that one satisfy two conditions: the induced metric must be continuous, and the extrinsic curvature must be continuous; or that for any discontinuity we have an energy momentum tensor which describes what needs to exist on the boundary for Einstein's equations to be satisfied. As long as it doesn't violate any energy conditions, the matching can, in principle, work.

As in the null matching case, we define intrinsic coordinates on the hypersurface, and by parametrization of the coordinates, tangent vectors. This gives us the induced metric along the hypersurface, which can be checked for continuity. Similarly to determining the transverse curvature in the null match, we determine the extrinsic curvature of the hypersurface. If the extrinsic curvature is not identical on both sides of Σ, there will be a shell of matter whose energy-momentum can be defined by the discontinuity in the extrinsic curvature. Further details of

this matching formalism, and an example of it, are in Appendix A.

Chapter 4

Primordial Structures

The primary interest of this thesis is in a scenario that is based on objects theorized to have formed in the early universe. In order to motivate the understanding of wormhole evaporation, it is important to discuss what have usually been considered the formation mechanisms of BHs, and other possible 'primordial' structures from the early universe.

4.1 Black Hole Formation

Astrophysically-created BHs are generally considered to all have the same basic formation mechanism – the collapse of sufficiently large mass such that after collapse it becomes a BH rather than something else like a planet, star, or neutron star. Typically, BH formation is considered to be one possible fate for a star at

the end of its life cycle.

Whether or not a star collapses to a white dwarf, neutron star, or a BH after a supernova (or other stellar end-of-life event) depends upon its size. Absent fusion, there is a balance between degeneracy pressures and gravity that maintains hydrostatic equilibrium. The mass limit beyond which gravity overtakes the pressures and the object becomes a BH is around 4 solar masses, a value calculated from the Buchdahl limit from fluid pressure [8]. Another boundary is the lower limit of electron degeneracy pressure which is known as the Chandrasekhar limit. It is around 1.4 solar masses, and is the maximum mass of a white dwarf, above this limit are neutron stars [35]. This limit is named for Subrahmanyan Chandrasekhar, but it's interesting to note that two other physicists, Wilhelm Anderson and Edmund Stoner, discovered it independently around the same time (1929-1931) [12].

Stellar BHs are limited in their minimal size at formation due to physical laws other than gravity; but BHs may in principle exist at any size based on general relativity because any object compacted in size to within its Schwarzschild radii will become a BH. BHs that are formed before the possibility of stellar collapse are called Primordial Black Holes (PBHs). They would have been formed in the early universe, and there are a number of proposed formation mechanisms as well as ongoing discussions about detection of PBHs that could be evaporating now [1].

The first suggestions of PBH formation came from Zel'dovich and Novikov

in 1966, and Hawking in 1971, with their formation originating from metric perturbations [77, 38]. Much work has been done since looking at other mechanisms such as density fluctuations, phase transitions, inflation, and others [48, 16]. BHs radiate with temperature

$$T = \frac{\hbar c^3}{8\pi G M k} \approx 10^{-7} \left(\frac{M}{M_\odot}\right)^{-1} \text{K}, \tag{4.1}$$

where we have the usual constants and the mass, M, of the BH, with $M_\odot$ denoting a solar mass. The timescale of evaporation is therefore

$$\tau(M) \approx \frac{\hbar c^4}{G^2 M^3} \approx 10^{64} \left(\frac{M}{M_\odot}\right)^3 \text{y}, \tag{4.2}$$

so the only BHs that could be evaporating now would have masses of 10^{15}g. Therefore this means only BHs formed during the first 10^{-23}s, because the mass,

$$M_H(t) \approx \frac{c^3 t}{G} \approx 10^{15} \left(\frac{t}{10^{-23}\text{s}}\right) g \tag{4.3}$$

is dependent on the particle horizon at the time of their formation [16]. Detection of this evaporation would be difficult but not impossible. Khlopov and Carr [48, 16] provide a good review of the state of the field theoretically. There are multiple ongoing experiments testing possible observability of PBH evaporation, which are summarized in [1].

4.2 Inflation

One possible era that could produce PBHs is the inflationary epoch. Inflation is a framework that was originally synthesized by Alan Guth [34] as a way to explain the "initial" conditions of the Big-Bang cosmology more satisfactorily than simply posing them by fiat.

Inflation is an exponential expansion of space, generally assumed to be driven by one or more scalar fields. If inflation is sufficiently long-lived, it leads to a very homogeneous, isotropic, and flat early state that is compatible with our observations of the Cosmic Microwave Background (CMB) [70]. Inflation solves the observational problems laid out below.

When we look out, we see that our universe is expanding (in an accelerated fashion), and we can see back to the CMB, the farthest back visible, opaque light surface. It is surprisingly homogeneous and isotropic. We have to explain the homogeneity and isotropy (the horizon problem), the large scale structural and particle evolution of the universe and also initial velocities (flatness problem) [70]. Inflation is a period of exponential expansion of space after the big bang, an epoch that lasted from $10^{-36}s$ to $10^{-32}s$.

The horizon problem is that regions that are causally disconnected in our universe are homogeneous and isotropic, and appear to be in thermal equilibrium. Therefore there needs to be mechanism through which all points in our present

horizon were once close enough to each other to be in thermal equilibrium, and changed fast enough to not disrupt that. The flatness problem deals with the fact that the density of matter is very even across our universe, and fits the parameters necessary for it to be flat. Without inflation it would appear we would need fine tuning to get a flat spacetime.

There is also the issue of magnetic monopoles, which theoretically are predicted to exist by GUT theories, but we do not see them. Inflation can make it so that it would be so rare to find one that our observations would be expected.

Inflation also gives us an intrinsic mechanism from QM to leave density perturbations, and the statistics of these beautifully match the form (though not very naturally the amplitude) of perturbations seen in the CMB. Inflation has enjoyed fairly widespread acceptance due to its predictive and explanatory success. Still, there are some proposed and considerably less popular alternatives [69, 3].

Since the mechanism for PBH formation we will be focusing on is based on inflation, we present a couple definitions that are sourced from Mukhanov's textbook on cosmology [70]. The background spacetime is the Friedman Lemaitre Robertson Walker metric

$$ds^2 = -dt^2 + a^2(t)\left(\frac{1}{1-kr^2} + r^2 d\Omega\right). \tag{4.4}$$

where $a(t)$ is the scale factor and k is spatial curvature. Inflation is defined by

the inflaton field lagrangian

$$\mathcal{L} = \frac{1}{2}\dot{\phi}^2 + \frac{1}{2}g^{ij}\partial_i\phi\partial_j\phi - V(\phi), \tag{4.5}$$

where we have a scalar field ϕ, the spatial metric g^{ij}, and the inflation potential $V(\phi)$.

4.2.1 Bubble Universes

If the inflaton potential $V(\phi)$ has an interesting structure, it can in turn support some additional interesting processes beyond exponential expansion. One of these properties is "bubble formation" in which a spherical region of relatively lower vacuum energy nucleates and grows within a region of relatively higher vacuum energy [19]. These bubbles have been considered in cosmology as "universes" as they can be seen as spatially infinite inside, and if inflation occurs inside a bubble, then the bubble could contain a viable big-bang cosmology, even while other such bubbles exist elsewhere as different "universes."

The bubble structure is such that the two phases are separated by a spherical bubble wall (a sort of domain wall) containing both trapped potential energy as well as kinetic energy of expansion driven by a difference in pressure on each side (outward if higher vacuum energy on the outside than on the inside). Whether formation occurs and how a bubble forms depend upon the structure of the potential. The bubble must form large enough that the volume of energy

remaining in the interior can supply the potential energy trapped in the bubble wall. Bubbles can also collapse if the pressure gradient is inward (i.e. higher vacuum energy on the inside.)

4.3 Primordial Wormholes

A new set of PBH formation mechanisms were introduced by Garriga et al., originating from the collapse of inflationary bubble universes and domain walls [32]. Both scenarios were laid out in more detail in separate follow up papers by Deng et al. [24, 23]. Their mechanism for the collapse of inflationary bubbles into BHs has two possible outcomes, depending on the mass, which is defined through a number of inflation dependent parameters. One outcome resembles the BH remnant of usual stellar collapse. In the other, the resulting BH is on one side of an ER bridge that connects our Universe with an inflating universe. Because the creation of a "baby universe" of this type is very difficult [29, 2], this result is remarkable and deserves further consideration, motivating the study here.

The basic idea is as follows. Bubble nucleation is exponentially suppressed when going from low to high-vacuum energy [2, 52, 47, 75]. As a result, bubble nucleation typically *decreases* vacuum energy, leading to an outward pressure gradient that causes bubble to expand. In Garriga et al.'s scenario, inflation has two field directions, and while tunneling occurs in one direction, the field can still roll

in the other. Thus a bubble can form with a decrease in vacuum energy, yet *after* formation, due to the rolling field, the relative vacua can switch so that the bubble feels an inward pressure gradient and collapses to a BH.

In the model worked out by Garriga et al., inflation ends and at $t = t_i \sim H_i^{-1}$ (where H is the Hubble constant) and we have an FRW universe that is connected to a collapsing de Sitter (dS) bubble, junctioned to a Schwarzschild-de Sitter (S-dS) for the BH which is itself connected to the FRW by a shockwave emanating from the collapse. The mass parameter for the BH is defined as

$$M_{bh} = \frac{4}{3}\pi\rho_b R^3 + 4\pi\sigma R^2 \left[\dot{R}^2 + 1 - H_b^2 R^2\right]^{1/2} - 8\pi^2 G\sigma^2 R^3, \tag{4.6}$$

where the vacuum density inside the bubble is ρ_b, σ is the bubble wall tension, and R is the bubble radius. Also, we have $\dot{R} \equiv dR/d\tau$, where τ is the proper time for the bubble wall. Using the initial condition $\dot{R} \approx H_i R_i$ and end of inflation time this simplifies to

$$M_{bh} \approx \left(\frac{4}{3}\pi\rho_b + 4\pi\sigma H_i\right) R_i^3. \tag{4.7}$$

We can now look at this for the two possible collapse scenarios: subcritical and supercritical bubbles. The critical mass parameter is approximated by the Hubble parameters of the vacuum bubble interior and the bubble wall

$$GM_{\rm cr} \sim \min\left\{H_{\rm b}^{-1}, H_\sigma^{-1}\right\}, \tag{4.8}$$

meaning bubbles with a mass lower than this will entirely collapse and bubbles with a larger mass will continue to inflate.

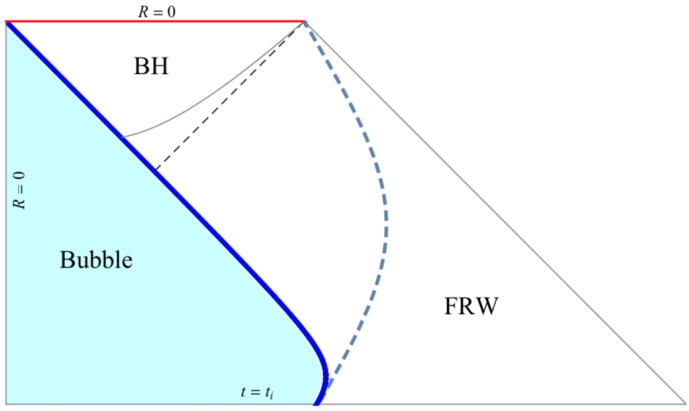

Figure 4.1: Conformal diagram of a subcritical mass BH. Here the teal bubble collapses, with blue bubble wall heading to $r = 0$, outside FRW is connected to Schwarzschild via the propagating shock wave denoted by blue dashed line. The BH has two horizons indicated, the coordinate event horizon is dashed and the apparent is solid. Source: Deng et al.[24]

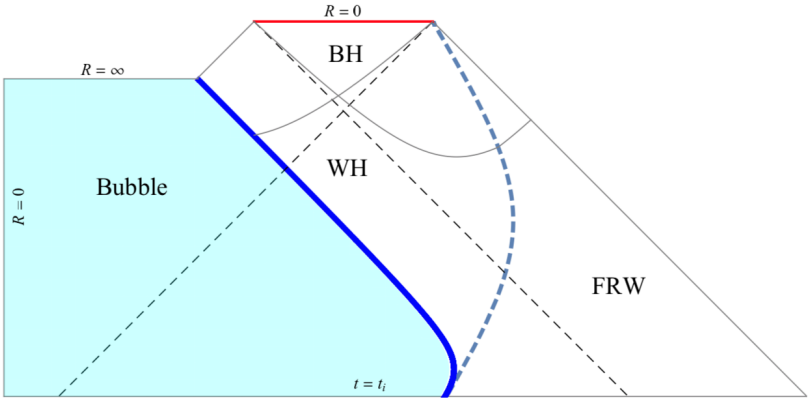

Figure 4.2: Conformal diagram of a supercritical mass black hole. The teal bubble collapses, with blue bubble wall now continuing to inflate. outside FRW is connected to Schwarzschild via the propagating shock wave denoted by blue dashed line as in the subcritical case. The BH again has two types of horizons indicated; the coordinate event horizons are dashed and the apparent horizons are solid. We also see an ER bridge and part of the white hole side of Schwarzschild, making the wormhole traversable for a fixed proper time. Source: Deng et al.[24]

Subcritical bubbles collapse into a regular BH as shown in figure 4.1 with the resulting BH mass

$$M_{bh} \approx \frac{4}{3}\pi\rho_b R_{\max}^3 + 4\pi\sigma R_{\max}^2 \tag{4.9}$$

where $R_{\max}$ is the maximum radius the bubble achieves before it collapses. Supercritical bubbles have a different structure, maintaining their ER bridge and are traversable for a period of time. This means worldlines in the FRW region can causally reach the other side of the bridge (as can be seen in figure 4.2.) The wormhole closes after $t \sim GM_{bh}$. Using numerical simulations, Deng et al. found supercritical BH masses to be

$$GM_{\rm bh} \sim H_i R_i^2. \tag{4.10}$$

The mass spectrum of these BHs is quite wide and constrained by observational data as well as amplitudes of inflationary perturbations. We are interested in the ones formed from supercritical bubbles that contain an ER bridge. It is possible that these BHs become the seeds for the supermassive BHs we see at the center of galaxies [24].

This BH formation mechanism is fascinating because it presents a natural formation scenario for a Schwarzchild wormhole, and offers a possible physical basis for a Schwarzchild wormhole in our universe. It is reasonable to look at this mechanism with a bit of care since it is suggesting something that has not

previously been seriously considered: the existence of the extended Schwarzschild metric as a physical reality.

The study of evaporating wormholes as a theoretical process is of some interest in its own right. But the formation of BHs and an ER bridge from vacuum bubbles, and with it the suggestion we might have them in our universe, adds significant impetus to studying processes such as evaporation that are involved in such objects, but may have been largely neglected before. However, it is interesting to note that, quite independently, there have been other recent conversations around wormholes and their formation mechanisms; but these have come mostly from theoretical explorations such as modified gravity, which are not immediately relatable to our universe [5, 13, 63, 9, 33, 44, 68].

Chapter 5

Black Hole Evaporation

5.1 Hawking Radiation

Hawking's original calculation indicating that BHs would have a temperature is based on QFT in curved spacetime. He showed that a quantum field theory vacuum state in which there is no radiation at early ($t \to -\infty$) times, and finite energy density on the horizon, necessarily leads to outgoing radiation at late ($t \to +\infty$) times [36]. An interpretation of this – borne out by subsequent calculations – was that particle creation and annihilation occurring near a BH horizon would result in the horizon driving the process, sending a negative-energy flux into the BH and a positive one outward [21]. The energy momentum tensor for the radiation flux was not presented by Hawking, but by Fulling, Davies, and Unruh, and need not necessarily be looked at as particles [31, 20, 73]. Since then, there have been alter-

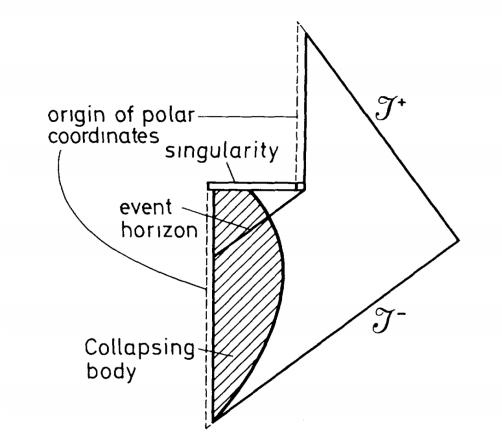

Figure 5.1: Original Penrose diagram of an evaporating BH presented by Hawking in his 1974 paper "Particle Creation by Black Holes." Source: Hawking [36]

native descriptions of how the evaporation and particle escape would occur, with the WKB tunnelling picture being widely used (see Appendix B for an overview).

As mentioned in the introduction, there has been much controversy over the implications of Hawking Radiation; indeed, his arguments have essentially spawned a whole field of inquiry for what is now approaching 50 years. Something that has not changed significantly, however, has been the use of the Penrose diagram originally put forward, seen in figure 5.1. This diagram, while widely adopted, fails to convey several crucial considerations in the process as well as "building in" the sort of information loss initially advocated – but later repudiated – by Hawking.

5.2 Modeling Evaporation

The inaccurate and "hand-drawn" nature of diagrams representing the Hawking process motivated us (in SAK [65]) to formulate a mathematically accurate classical, or at least semi-classical, diagram that we can reference when considering the many open questions and postulated theories surrounding BH evaporation. Using the matching methods introduced in chapter 3, and ensuring that they were sufficient to model descriptions of Hawking radiation, we developed a methodology for plotting accurate diagrams. Schindler developed algorithms and a suite of python codes to produce these diagrams [64]. This section describing the modeling methodology is mostly comprised of direct excerpts from SAK, presented here with permission [65].

This model cannot fully encapsulate the details of the evaporation process, especially since the diagram is based in classical general relativity while evaporation is an inherently quantum process; and it has no means to represent quantum gravity effects or even regions governed by quantum gravity. The assumptions of the method are as follows [65]:

1. The black hole is non-rotating and spherically symmetric.

2. The process is quasistatic, allowing dynamical evolution to be modeled by a sequence of equilibrium BH solutions joined across null shells of matter

(such null shells may represent either truly light-like radiation, or highly accelerated timelike matter).

3. The equilibrium black hole solutions locally have the form $ds^2 = -f(r)\,dt^2 + f(r)^{-1}\,dr^2 + r^2\,d\Omega^2$.

4. Stellar collapse and mass accretion is modeled by a sequence of ingoing spherical null matter shells, incident from infinity.

5. Hawking radiation is modeled by pairs of spherical null matter shells. Each pair consists of an outgoing positive-mass shell and ingoing negative-mass shell. Each pair nucleates at a fixed radial distance l_{ev} outside the apparent horizon, with both shells propagating toward the future. Nucleation points violate the DTR relation (an equation related to energy conservation, see appendix), but the amount of violation is arbitrarily small in the $l_{ev} \to 0$ limit. If $l_{ev} \approx l_{pl}$, tiny DTR violations may be considered small quantum fluctuations. In this sense – in our semi-classical model – energy conservation forces Hawking radiation to be emitted from just outside the horizon.

This model is a slightly generalized, discrete approximation of the model proposed originally by Hayward [41], and the evaporation mechanism agrees, heuristically, with the classic calculation by Davies, Fulling, and Unruh of the stress tensor for a quantum scalar field in the presence of a static BH [21]. We construct space-times applying this model, and construct their corresponding Penrose diagrams

by the methods of Schindler [64]. It is assumed that physically realistic models are achieved by first taking the limit $l_{ev} \to l_{pl}$ at each shell of Hawking radiation, then taking the continuous (many-shell) limit.

5.3 Penrose Diagram

By applying the model above, we can produce Penrose diagrams. The following diagrams and descriptions are from SAK [65].

Penrose diagrams of singular and non-singular BHs generated per the above assumptions are shown in figure 5.2. Parameters are chosen to illustrate qualitative features, but the time evolution and relative length scales are not realistic.

Positive-mass (accretion and outgoing Hawking radiation, gray dashed) and negative-mass (ingoing Hawking radiation, gray dotted) shells separate the spacetime into piecewise regions, with Hawking radiation nucleating at a tiny radial distance l_{ev} outside the horizon of the region to its past.

The curvature cutoff length scale l (which has physical significance only in Hayward regions) is held fixed across all regions, while the mass parameter m (which in every region determines the gravitational mass measured by a distant observer) varies.

The total mass M is the maximum value of m in any region, and locally

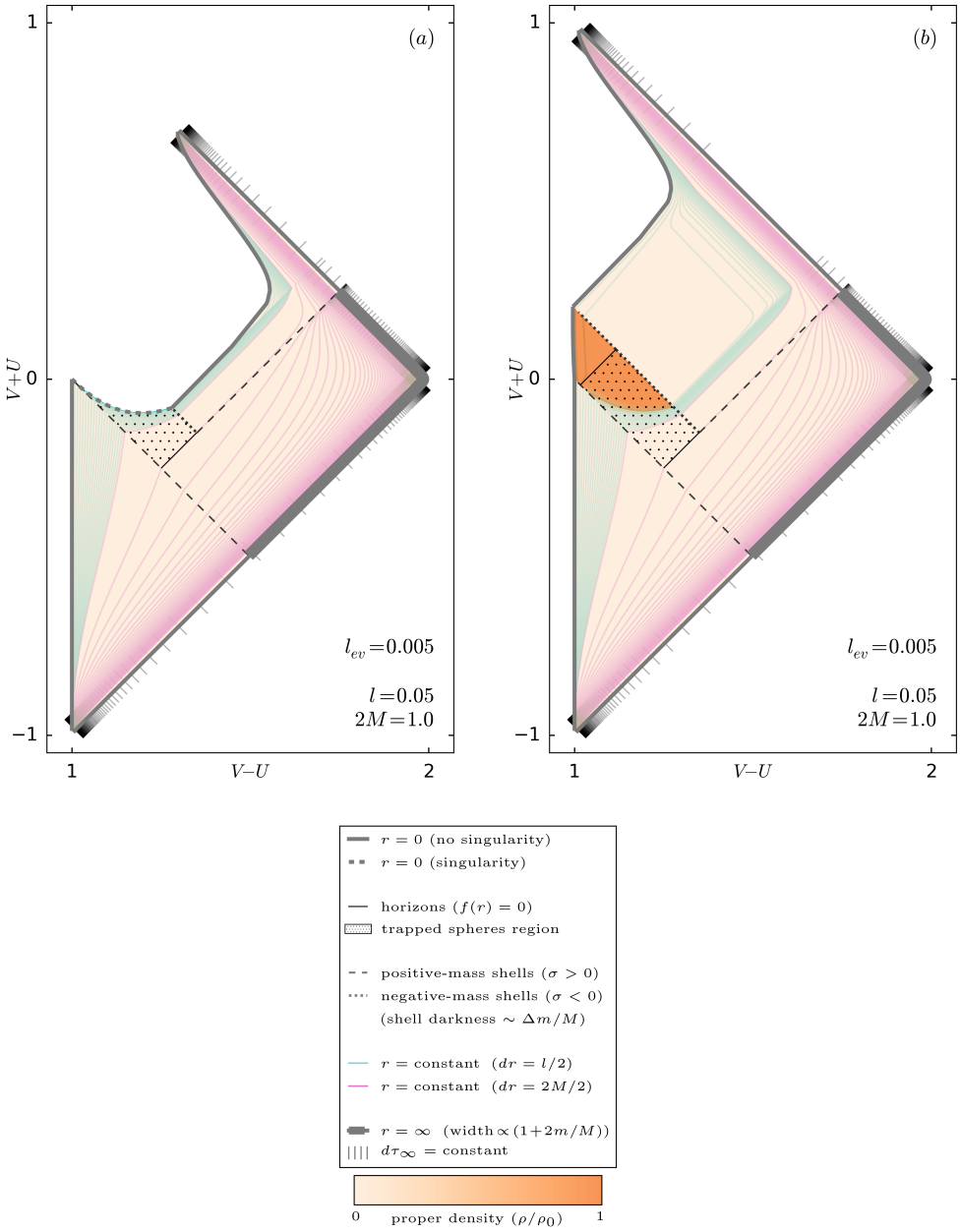

Figure 5.2: Penrose diagrams for (a) singular and (b) nonsingular black holes which form by accreting a single shell of infalling matter and evaporate by emitting a single blast of Hawking radiation. Source: J. Schindler, A. Aguirre, & A. Kuttner [65].

m is visualized by the linewidth of the conformal boundary at $r = \infty$ in each region (linewidth proportional to $1 + 2m/M$).

Tick marks (gray) along $r = \infty$ mark off equal increments of proper time for an infinitely distant observer at constant radius (i.e. constant increments of du and dv along null infinity). The trapped spheres region (black dot-hatch fill), bounded by horizons (black) where $f(r) = 0$, contains closed trapped spheres. Background coloring is determined by the local proper density ρ (orange color scale), scaled by the maximum density $\rho_0 = 3/(8\pi l^2)$.

The Hayward core is clearly visible as a dark orange region in the density plot, and the core surface almost exactly corresponds to the singularity location in the Schwarzschild case. Notably, distant observers near future null infinity begin to observe Hawking radiation at the same moment they see the infalling accretion shell fall through its own horizon.

Lines of constant radius are shown at small ($dr = l/2$, teal) and large ($dr = 2M/2$, magenta) length scales; even where they appear bundled or strongly kinked, they do in fact remain continuous.

One strange-looking feature of this diagram is the appearance of a set of wiggly kinks and a few stray tick marks to the future (measured along future infinity) of the final evaporation shell, before the very stretched out area. These are artifacts of the unrealistic parameters, and in more realistic models these kinks and tick marks all coincide with the final shell.

Coordinates V and U, which define the axes, are arbitrary null global coordinates, defined further in Schindler [64]. For in-depth analysis of these diagrams, see SAK [65]. Not shown here are diagrams showing multiple formative and evaporative steps, rather than only one each way. For our purpose, the most important thing to gain from these diagrams is that the methodology given for modeling evaporation can produce the pictures we want of evaporating wormholes. The diagrams that are produced are sensible and cover important features of the BH evaporation process that can then be analyzed. We can now apply this model to other scenarios, including wormhole evaporation and the construction of many other spacetimes.

Chapter 6

Wormhole Evaporation

As far as the spacetime outside is concerned – and presumably the fields in it – there is no difference between a "standard" BH and one that constitutes one end of an ER bridge. Thus insofar as calculations indicate that a BH formed via "standard" means evaporates, those calculations also imply that an ER bridge wormhole should evaporate.

Based on the explicit model and computation of BH evaporation from SAK [65], we can examine what an evaporating extended Schwarzschild (ER bridge) spacetime would look like. This process could possibly occur in our universe, as it also underlies the Garriga et al. setup [32, 24] of BH formation via inflationary bubbles. We will return to the larger issue of wormholes possibly existing in our universe and what their evaporation would look like; but for now we will undertake the mathematical experiment of evaporating a purely (extended)

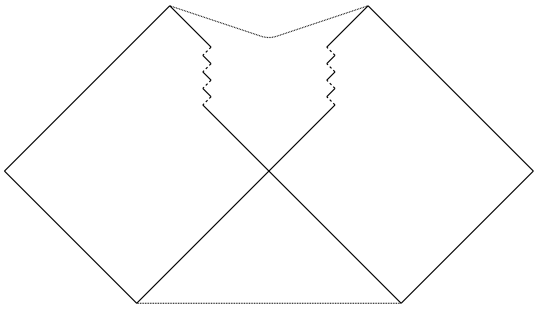

Figure 6.1: Basic cartoon sketch of multiple steps of evaporation on both sides of an extended Schwarzschild.

Schwarzschild BH.

There are two questions to look at in terms of wormhole evaporation. First is the question of what happens as it is evaporating, much as for a BH: what is the causal structure of the spacetime and how should the overall process be best understood? The second is that of the system's final state. This is a somewhat different question from the usual BH evaporation because there are two – rather than one – large spacetime(s), in which two – rather than one – object(s) exist and evaporate. After regular BH evaporation, there is one Minkowski space, potentially with a BH remnant. So there is a basic question of whether after ER bridge evaporation there are two disconnected regions (possibly each with a remnant) or one still-connected spacetime.

Following the same basic model in which we treated BH evaporation – ingoing and outgoing null shells representing radiation – we treat the problem of

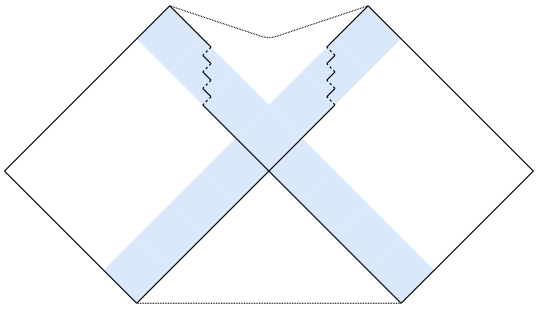

Figure 6.2: Cartoon demonstrating traversable regions opened up by evaporation of both sides of an extended Schwarzschild wormhole.

two equal-mass BHs on the two ends of the ER bridge, evaporating at the same rate. The qualitative result of such a process – depicted in figures 6.1 and 6.2 – can be seen even without any calculation. It is clear that once a shell has evaporated (on one side or both), in effect making the horizon timelike, the wormhole becomes traversable. We can see that either universe can send signals through to the other if both sides evaporate. (Or if somehow only one side evaporated, the opposing side can send signals through to the evaporated side.) The importance of this qualitative effect is clearly determined by the parameters of the evaporation; to understand that, we must first calculate the feasibility of the evaporation with the DTR relation and then look at how a signal might travel through. We also note that just as evaporation makes the horizon effectively timelike, accretion makes it effectively spacelike, and for traversability to occur it is clear that there must be net evaporation, meaning evaporation must outweigh accretion.

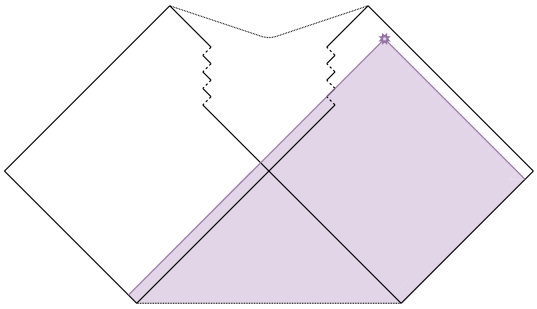

Figure 6.3: Cartoon of Schwarzschild evaporated in steps. The purple star represents an observer in the righthand universe, and the shading is their past lightcone that would ostensibly be visible to them. The steady shrinking of the Schwarzschild radius renders the (apparent) horizon timelike.

6.1 Traversability

Given that an evaporating wormhole is formally traversible in terms of its causal structure, it is important to ascertain whether something stands in the way of signals being sent from one side to the other. Consider, for example, an obersver as marked in figure 6.3, with a past light cone as marked in purple shading. Can a signal originating in the region inside the past lightcone in the other "universe" traverse the wormhole without disrupting it?

Our process will go as follows. First, we must show that if we evaporate a step in extended Schwarzschild or Hayward, it works with shell matching and satisfies the DTR relation. Then we will look at what happens if a spherically symmetric signal from one universe goes through the traversable section into the

other universe, approximating it as a small energy shell. We will also look at redshift and blueshift of the signal to see if it is visible. Note this does not address if these signals would be observable in a meaningful way, simply if they theoretically cross from one universe to the other meaning the wormhole is formally traversable; we will touch upon observability later.

We begin with the general calculation for a step of evaporation reducing the mass of the BH from M_1 to M_2, modeled as shells departing the horizon of the M_1 Schwarzschild BH, leaving a region in section A of the DTR corner junction, from figure 3.3, of Schwarzschild with M_2, the others still M_1. Using the DTR relation from equation 3.18, we can find at what value of r_0 we may match so that energy is conserved; so we have

$$\left(1-\frac{2M_2}{r_0}\right)\left(1-\frac{2M_1}{r_0}\right)=\left(1-\frac{2M_1}{r_0}\right)\left(1-\frac{2M_1}{r_0}\right). \tag{6.1}$$

Rearranging for r_0 we find

$$r_0=\frac{2(M_2M_1-M_1^2)}{M_2-M_1}. \tag{6.2}$$

Since we are calculating this for a scenario where we are decreasing M_1 by a small step, we can say $M_2=M_1-\delta$, so by replacing M_2 we can further simplify as

$$\begin{aligned} r_0&=\frac{2((M_1-\delta)M_1-M_1^2)}{(M_1-\delta)-M_1}\\ &=\frac{2(-\delta M_1)}{-\delta}, \end{aligned} \tag{6.3}$$

and we see that DTR is satisfied if $r_0=2M_1$; or in other terms, the matching and

evaporation takes place along the horizon of the original BH; this was noted also in SAK [65].

The appropriate evaporative matching therefore is along $2M_1$. The shell junction between M_1 and M_2 results via equation 3.15 in the energy density of the evaporation shells being

$$\sigma_{evap} = \pm\frac{M_2 - M_1}{4\pi r^2}, \tag{6.4}$$

which will be overall negative for the ingoing shell and positive for the outgoing one, which is sensible as the mass is decreasing ($M_2 < M_1$).

Using the algorithms developed by Schindler [64], plotting an example of the step from Schwarzschild to a smaller Schwarzschild appears as in figure 6.4 with lines of constant r in figure 6.5. As expected, the causal structure, indicating that a signal can travel from the "left" region to the "right" (observed) region, remains.

Given this causal structure, an important question to investigate is whether a physical signal (carrying energy) can pass from one side to another without disrupting the structure. After all, an incoming signal constitutes energy that should add to the BH mass and expand the horizon. On the other hand, the signal *leaving* the BH decreases the horizon size again.

To gauge these effects, we now turn to calculating the matching and DTR relation for a signal leaving an event in the opposing universe of the ER bridge

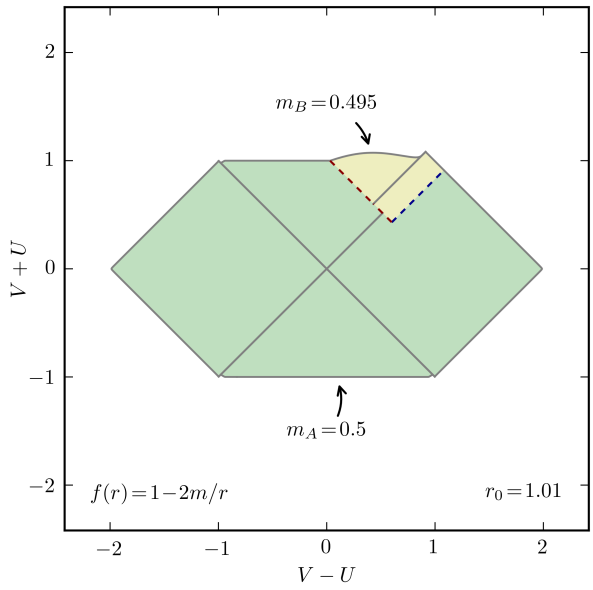

Figure 6.4: Schwarzschild with one evaporative step on one side only. Conformal coordinates are listed on the axes, and the mass change is shown. Source: provided by J. Schindler.

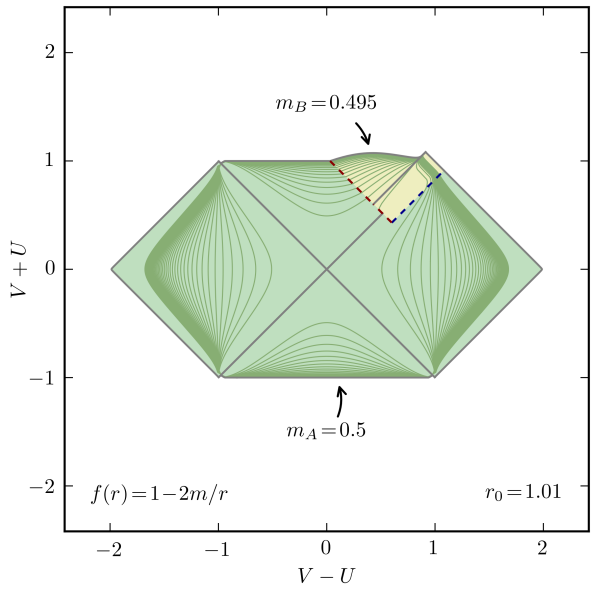

Figure 6.5: The same Schwarzschild evaporation diagram as in figure 6.4 with lines of constant r added in. One can see how they match at the boundary. Source: provided by J. Schindler.

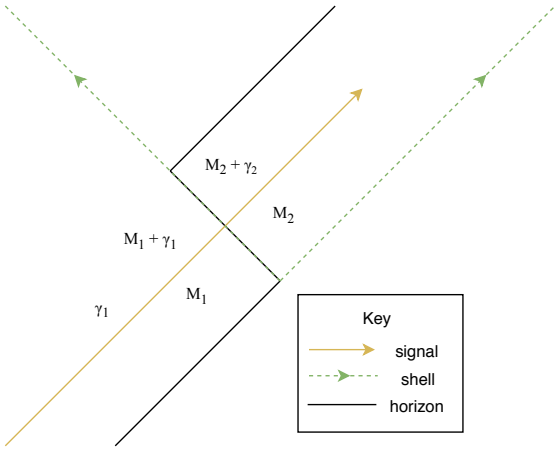

Figure 6.6: Sketch of a signal crossing an evaporative step, with regions indicated with their mass parameters for calculation.

and travelling through to where the wormhole has decreased in size, traversing the evaporation energy density, and out into "our" universe (here assuming we treat the right hand side as our side and the left as the opposite). We imagine the signal as an S-wave spherically symmetric "photon" pulse, modeled as an incoming or outgoing spherical null shell. Figure 6.6 shows a schematic of the matching where an event sends a signal through the wormhole.

For this calculation, we denote the starting photon mass equivalency (by which we mean the increment in BH mass that would occur simply by accreting the photon, per Eq. 6.4) by γ_1. For the radius where the photon crosses out of the wormhole we will use the halfway point between the Schwarzschild radii for M_1 and M_2, at $r = M_2 + M_1$. For the DTR matching (as in part (a) of figure 3.3, applied to figure 6.6), region A has unknown mass parameter $(M_2 + \gamma_2)$, region C now has M_2, while region B has M_1, and region D is $M_1 + \gamma_1$. The DTR matching

at the intersection of $r = M_2 + M_1$ and the incoming (negative) mass shell is therefore

$$\left(1 - \frac{2M_1}{M_2 + M_1}\right)\left(1 - \frac{2(M_2 + \gamma_2)}{M_2 + M_1}\right) = \left(1 - \frac{2M_2}{M_2 + M_1}\right)\left(1 - \frac{2(M_1 + \gamma_1)}{M_2 + M_1}\right), \tag{6.5}$$

which simplifies to

$$\frac{-\gamma_2}{M_1 + M_2} + \frac{2M_1\gamma_2}{(M_1 + M_2)^2} = \frac{-\gamma_1}{M_1 + M_2} + \frac{2M_2\gamma_1}{(M_1 + M_2)^2}. \tag{6.6}$$

Multiplying the squared denominator through reduces it to

$$\gamma_2 = -\gamma_1. \tag{6.7}$$

Note that this is exact and does not require γ_1 or γ_2 to be small.

This result shows two things. First, in terms of the photon's energy density, crossing from inside to outside of the Schwarzschild radius is precisely when the photon goes from being ingoing to outgoing. Therefore the ϵ (c.f. Eq. 3.15) switches sign too, so that

$$\sigma = \frac{\gamma_1}{4\pi r^2} \tag{6.8}$$

is the (thus positive) energy density of the photon shell for both sides of the junction. Therefore the photon energy is unaffected crossing the horizon and the evaporative energy density.

Second, we see that BH mass increases due to the signal do occur, but on the *left* side of the bridge. On the other hand, the mass after the photon leaves,

$M_2 + \gamma_2 = M_2 - \gamma_1 < M_2$ results in *lowering* the mass of the the BH. So the mass equivalency of the photon's energy does not "close" the wormhole.

Although the signal's energy is unaffected by crossing the ingoing shell, it is of course affected by gravitational blue/red shift. The ratio between frequencies for a photon between two points in Schwarzschild can be calculated as

$$\begin{aligned} \frac{\omega_2}{\omega_1} &= \frac{\Delta\tau_1}{\Delta\tau_2} \\ &= \left(\frac{1-2GM/r_1}{1-2GM/r_2}\right)^{1/2}, \end{aligned} \tag{6.9}$$

where the ω are the (angular) frequencies, and the τ are proper times [17]. In our case of an event in the opposing universe, we can apply it to a photon coming from the event to the crossover point, and then again to the photon once it has exited the wormhole and travels to large r to be observed. Given the crossing point is not going to be properly defined, we have to do each side separately and understand the above matching calculation to show the signal is unchanged across the boundary. We have been working with photon mass equivalency, which is its energy, since $E = hf = \frac{h\omega}{2\pi} = \hbar\omega$, so a ratio of frequencies is equal to a ratio of energies so we may use

$$\frac{E_2}{E_1} = \left(\frac{1-2GM/r_1}{1-2GM/r_2}\right)^{1/2}, \tag{6.10}$$

where the radii correspond to starting and finishing positions, and the mass is of the Schwarzschild mass of whichever region the radii correspond to on either side. This should be computed on the side that is observed in an observer lightcone.

Unless the mass ratio is very extreme, this energy ratio can always be counteracted by choosing appropriate radii r_1 and r_2; so it does not seem that this provides any fundamental limit to signaling through the bridge (as it would, for example, if there were a divergence in the redshift factor.)

We conclude that the wormhole is traversable after shells have evaporated, and that signals can in fact get through from one side to the other without "closing" the wormhole or being redshifted into oblivion. Because the result is independent of photon mass, we can consider a very high energy/short wavelength modulation of radiation passing through, potentially carrying significant information.

6.2 Final Evaporation

A second very interesting question that comes to light regarding wormhole rather than BH evaporation is that of the post-evaporation spacetime. Insofar as this has been considered in the past, it appears to have been generally assumed that bubble universes pinch off so that there are two completely separated universes [14]. It is, however, quite unclear how that could happen at the classical or semiclassical level; there is no continuous path from a spherically symmetric spacetime with *no* origin into one with two different origins.

On the other hand, it is at least, in principle, reasonable to transition

from an ER bridge into a traversible wormhole solution like the Ellis solution, so we have examined this as a potential transition.

The Ellis wormhole is not SSS, and therefore in order to follow the DTR matching relation, we need to put the metric in the form of equation 3.19.

We wish to write the Ellis metric of Eq. 2.11:

$$ds^2 = -dt^2 + dr^2 + (r^2 + n^2)d\Omega^2 \tag{6.11}$$

in the form of Eq. 3.19:

$$ds^2 = -e^{-2\phi(r)}f(r)dt^2 + f(r)^{-1}dr^2 + r^2 d\Omega^2. \tag{6.12}$$

If we replace $r^2 + n^2$ with r'^2 and then $r' \to r$ we get

$$ds^2 = -dt^2 + \left(\frac{r^2}{r^2 - n^2}\right) dr^2 + r^2 d\Omega^2, \tag{6.13}$$

so we can have

$$f(r) = \frac{r^2 - n^2}{r^2} \tag{6.14}$$

which results in the correct form if we define $\phi(r)$ by

$$e^{-2\phi(r)}f(r) = 1. \tag{6.15}$$

Now we can use the DTR relation 3.18 with the more generalized metric form. We will use Hayward because the regularized interior was convenient for the BH matching, but the Schwarzschild case is essentially equivalent. We must satisfy the DTR relation at the evaporation point, r_{ev}, and at the central match

close to $r = 0$ which we denote by r_0. The evaporation point is the familiar matching we have shown before for evaporating shells, whereas the central match is where the two ingoing shells meet near $r = 0$. At r_h we have

$$\left(\frac{r_{ev}^2 - n^2}{r_{ev}^2}\right)\left(1 - \frac{2mr_{ev}^2}{r_{ev}^3 + 2l^2m}\right) = \left(1 - \frac{2mr_{ev}^2}{r_{ev}^3 + 2l^2m}\right)\left(1 - \frac{2mr_{ev}^2}{r_{ev}^3 + 2l^2m}\right), \tag{6.16}$$

which is satisfied with $f_h(r_{ev}) = 0$, which occurs at the horizon; and we see again that we have to match shells at the horizon. Now at r_0 we have

$$\left(\frac{r_0^2 - n^2}{r_0^2}\right)\left(1 - \frac{2mr_0^2}{r_0^3 + 2l^2m}\right) = \left(\frac{r_0^2 - n^2}{r_0^2}\right)\left(\frac{r_0^2 - n^2}{r_0^2}\right), \tag{6.17}$$

which is satisfied if we match at $r_0 = n$. It is interesting to note this also works for Schwarzschild on fundamental grounds, because the evaporation matching happens at the horizon (the singularity of the metric), and the central point is dependent on Ellis, not Schwarzschild. In the DTR relation for the horizon match it is the Schwarzschild metric function that goes to zero, and for the central match, the Ellis function goes to zero. This shows that both ER bridge spacetimes evaporate to Ellis.

We can also calculate the stress-energy tensor at the junctions by finding the energy density from equation 3.15. For Ellis, the mass term is $\frac{n^2}{2}$, and for Hayward, it is $\frac{mr^3}{r^3+2l^2m}$; so the change in mass terms gives us

$$\sigma_{out} = \frac{mr}{4\pi(r^3 + 2l^2m)} - \frac{n^2}{8\pi r^2} \tag{6.18}$$

for the outgoing shell, and opposite sign for the ingoing one. For Schwarzschild, this is much simpler since the mass term is just M, and we get

$$\sigma_{out} = \frac{2M - n^2}{8\pi r^2} \tag{6.19}$$

for the outgoing one, and again opposite sign if considering the ingoing shell.

Here we have shown that energy is conserved for a final evaporation step if the metrics are matched at the neck of an Ellis wormhole. Again, this does not happen if one tries to match onto Minkowski.

We cannot explicitly compute a Penrose diagram for this scenario using the method of Schindler [64], because Ellis is not SSS, so a cartoon is provided in figure 6.7.

In the course of writing up this study, we found that the transitions from Schwarzschild (or similar) to a traversible wormhole (Ellis/ Morris-Thorne) had been investigated by Hayward [40, 43] and differently by Simpson and Visser [68]. Although these studies concerned macroscopic negative-energy shells (rather than evaporation), the essence is very similar, and this lends additional credence to our suggestion that an evaporating ER bridge would result in an Ellis remnant, presumably with the final neck being Planckian.

Given that evaporation ends at the Planck scale and our matching scenario methodology is classical, we cannot make a firm statement as to whether or not the final state Ellis persists.

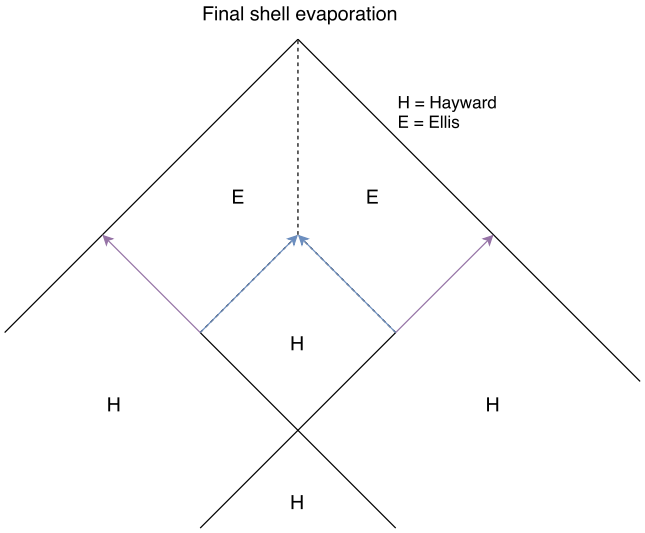

Figure 6.7: Hayward ER bridge evaporation to Ellis wormhole. Regions are labeled accordingly, blue lines are ingoing Hawking shells, purple outgoing, and the dashed line represents the wormhole neck.

It is important to note that the final evaporated remnant Ellis wormhole is sourced by an energy-momentum tensor that violates the weak energy condition – but only on a quantum scale, since the violation occurs at radius of order that of the neck, which is presumed to be of order the Planck length in an evaporated remnant.

6.3 Observability

We come to the consideration of whether an evaporating wormhole would be distinguishable from an evaporating BH that does not have an ER bridge. There are a couple of major things keep aware of, namely that the escaping signals change the wormhole mass – and differently on each side. But perhaps most importantly

for a signal to be seen, there has to be one coming through. This means there has to be something in the opposing universe that manages to send a signal into the BH. We use the term signal, but any source would work whose output entered the BH. We also looked at this evaporation scenario separately from its possible origin, so one would have to determine how seriously to take the options that predict the existence of wormholes.

One factor that would determine whether anything would be visible is if the signal flux would be discernible against the background of Hawking evaporation (given the BH is evaporating and thus has a temperature above the background) – and that is if there is even anything in other universes to shine through. The wormhole would also have to be observed at the right time. If there is a noticeable flux difference one could look to see if the spectrum is different. All of these factors place major limits on observability; and given our position, we cannot determine how many opposing universes would exist and what they might contain, or what the BHs did in our universe or the other.

It is interesting that given the nature of the opening created by the evaporation of a wormhole, it would only sometimes be possible to accrete radiation on to the BH, because much of the time it would just pass through. Whereas matter would tend to add to BH mass, without then subtracting from it on the way out.

A key consideration here is that when something collapses to form a BH,

the surface of that object turns into an infinitely redshifted surface (coincident with the horizon), so we lose information about what the BH used to be. On the other hand, for a wormhole there is no infinite redshift (as seen above in the collapse diagram description), therefore in principle the state of the other side could be probed.

There is also the fundamental question of whether or not an ER bridge can actually exist in our universe, but their existence is seeming more likely given the suggested formation mechanisms laid out by Garriga et al. and Deng et al. [32, 24]. The possible range of masses from collapsing vacuum bubbles is large, bounded primarily by observational constraints and by quantum scale interactions, which leaves room for the possibility that supercritical BHs are out there. If they seeded supermassive BHs we would not practically be able to observe their evaporation anytime soon.

With the span of theoretically existing wormholes and BHs across the age and size of the universe, it is possible for an evaporating wormhole to, at some point, have a noticeable signal come through from the other side, but we have no way of knowing this given our lack of knowledge about what other universes contain and because the signals also have to go into the BHs, which may have very small radii. There is the faintest hope that, if we detect evaporating BHs, they might have variation in their flux (and at a detectable level) and that would hint that there actually are differing types of BHs.

Another key question deserving of consideration is how detection of signals would work in the framework of general relativity. For instance, applying the work of Barrabes and Hogan on the detection of light-light signals and null shells [6].

Chapter 7

In our universe

Now that we have shown that an evaporating wormhole becomes traversable, and that at the end of its life it transforms into a wormhole remnant, something confirmed by other work showing an Ellis wormhole final state for an ER bridge [43, 68], we need to discuss the implications of these findings. Though it may be rather far-fetched that we could even observe a difference between a regular BH and a BH that is one side of a wormhole, there are theoretical questions that have been raised that warrant investigation.

7.1 Constraints

Some of the constraints on the possible existence of evaporating wormholes are enumerated in the previous section on observability, but they do not quite cover

everything. We emphasize the point that even though we showed traversability, we crucially have no way of knowing if it is typical for anything to occur in other universes. If we get to observe BH evaporation, we should look to see if there is variability of between signals from evaporating BHs. It is reasonable to think that signals altering their spectra would be rare and hard to detect, but again we do not know what happens in other universes, so we cannot know what to expect. The amount of signal is also greatly limited by multiple factors, as explained above.

The main suggested mechanism for the formation of ER bridge wormholes in our universe without exotic or new physics is from the collapse of vacuum bubbles [24]. However, there is reason to be careful about accepting this scenario without looking into it further. It is not immediately clear in the supercritical case what actually forms the mass equivalence when the BH collapses. Though the matching is mathematically sound, that does not mean it is necessarily physical. More investigation of this picture is needed, including double checking its topology, and ensuring that it satisfies the wave equation everywhere. We also note that the diagrams presented that describe the collapse scenarios do not include the whole past of the bubbles, in particular their creation [24].

7.2 Implications

Out of all the implications that arose, we found two of them to be especially pertinent. One is that it is clear worldlines can traverse out of this evaporating wormhole. The other is that what started a wormhole seemingly has to end a wormhole, as long as spacetime is treated classically, an evaporating ER bridge must form a remnant that looks like the Ellis spacetime or something similar.

Our wormhole evaporation mathematical experiment was done with the extended Schwarzschild and Hayward metrics. This means no formation mechanism is explicitly implied, as there is a white hole on the bottom of Schwarzschild. What was shown is that idealized signals can escape from a partially evaporated BH; but it is more complicated than that. Comparing this to the scenario of pure BH evaporation, there is no way of addressing where the information would be coming from. If we look at the vacuum bubble collapse formation scenario, the two universes began as one, and there is a region of the expanded bubble that cannot reach the BH. This means the information question may be entirely different here, but it is illustrative. Information can traverse an evaporated region if it can exist there.

The final state of our wormhole is another wormhole of Planck scale. In this case evaporating to flat space would not work. This outcome appears to indicate that the connection between universes does not get broken, and that the

wormhole structure is permanent unless/until quantum gravitational effects are taken into account. The apparently permanent connection raises the question of how it came to develop the wormhole structure, because ostensibly it should be reversible in terms of spacetime matching. Though our work resulted in a Planck scale Ellis wormhole, we cannot rule out other pictures or the possibility that the remnant may turn into something else or disappear by a mechanism not covered in the formalisms we used.

7.3 Open Questions

After this exploration, we are left with work to continue, but also a series of questions that arose from the research. As has been mentioned a few times, the feasibility of wormhole creation in our universe is an open conversation. Just because there is a metric for some spacetime does not mean it is physical in our universe and other methods of creation should be explored further.

There is a fundamental question of whether or not the extended Schwarzschild should be considered a physical possibility. As far as we knew, its formation had not been considered possible (at least via classical means), but now we have a possible formation scenario, so it is important to actually discuss the theoretical framework versus physical reality of these spacetimes. The mathematics shows it as a solution, and in other cases in physics (as with anti-matter's suggested

existence by Paul Dirac [25]) such solutions have turned out to have reality. But this does not tell us anything about how one might consider the mathematics of spacetimes, and work should be done on any proposed mathematical solution to confirm it as reality.

Early on we discussed the BH information paradox. While we do not suggest any remedies here, we do suggest that the implication of information escape in this scenario be considered and compared to stellar BH evaporation. In both cases, the information in question might be looked at as being contained in a singularity or core, and not the same as signals coming through. We believe it is also worth considering whether the concept of unitarity is well-applied to all BHs. The wormhole certainly did not begin as a closed system, and the universes are connected all the way through. We looked at the BH part of the way through evaporation, but that is not really a physical possibility. If a BH evaporates it does so all the way, so our example was simply for illustration, and no eternal BH of that form should be considered to exist in reality. Still, taking a dynamical view of evaporation as is done by SAK [65], would be beneficial. A proper evaporating wormhole the way we have figured it will always have an Ellis portion at the top.

The implication of the eternal wormhole remnant (or at least the prospect) would mean there may be permanent quantum scale WEC violations that necessarily accompany a non-evaporatable remnant. This may be acceptable but it might also cause problems when the universe is made up only of evaporating BHs

at the end of their lives.

Another interesting mystery relates to where the mass comes from to form the BH in the wormhole scenario. It appears that the extended Schwarzschild and the stellar collapse version both are defined with mass M. The question is therefore about the total mass of radiation to evaporate one compared to the other. Is mass M evaporated from both sides? If so, how can that make sense? Looking into this is one avenue of examining whether or not the extended Schwarzschild should be considered physical. Delving into the other ways Schwarzschild has been shown to reduce to Ellis would be a good place to start.

Many small curiosities remain, but the final big one we found has to do with evaporation rates. Hawking radiation should occur evenly as part of its definition, but that does not mean the accretion will be even on both sides of the BH, and it is far from clear what happens if an ER bridge accretes (or diminishes) differently in each universe. Where is the mass defined for each region based on lightcones and information? We would need to make sure not to violate information communication being within lightcones, and stay aware of how it relates to the shell matching mechanism. What happens if one side evaporates entirely and the other does not? Does it sit and wait? If so, this would have a noticeably different observable result than one that evaporates evenly. Or, perhaps, is there something that prevents the BH ends from changing size, so that they must evaporate evenly? We find these lines of questions fascinating and likely to illuminate

possible problems with these spacetimes.

7.4 Reasons to Believe

The primary reason to consider that these spacetimes could be physical is the growing literature suggesting that they do form, from some method or another, but a healthy dose of care and skepticism is always prudent. The number of publications regarding the formation of wormholes and even traversable wormholes is growing. It is turning out to not be such a far fetched concept, and there could be multiple ways for them to exist [5, 13, 63, 9, 33, 44, 68].

The examples of wormholes turning into Ellis that closely resemble ours are from Hayward [40, 43] and Simpson et al. [68]. They both look at Vaidya modeled shells of matter that grow and shrink wormholes. Simpson et al. look at a different situation called black bounce spacetimes, which have simply modeled evaporation to Morris-Thorne (Ellis).

Hayward has continued to work on wormhole dynamics and their energy condition violations, and even discusses Wormhole thermodynamics as a concept [42]. There are also other references to wormhole thermodynamics [46, 22]. It is important to note that we looked at the classical general relativistic side with approximations for the quantum effects, leaving other approaches alone.

At least for now, the testability of differentiating evaporating BHs seems

far fetched, though we have produced an ostensibly observable result if formation scenarios are realistic. We present our mathematical results here, as independently interesting, and as food for further study. Since our work on the final state of an evaporating BH is corroborated by others, we can assert with confidence that, if the ideas that suggest wormholes can be formed in our universe are confirmed, we have presented here how they will evaporate in an even evaporation scenario.

Chapter 8

Conclusion

Long relegated to solutions of purely mathematical interest, wormholes have lately found a resurgence of attention. Quantum scale interactions beckon us along, promising that what we once thought was impossible due to energy condition violations may now be possible; but only if we are playing in the right neighbourhood. Sometimes when one peels back layers of the theory, one is faced with interpreting an equation or diagram in order to bring it into the real world, and suddenly, even with assumptions laid bare, it is still unclear what is physical and what is not.

Part of the difficulty is that wormhole evaporation is, inevitably, part and parcel to *black hole* evaporation. There are a plethora of papers and theories attempting to explain or solve the BH information paradox and its new incarnation, the firewall paradox. The fray has gotten pretty messy. Our intention is to lend

some clarification to the situation. Our work untangling and computing a proper diagram for an evaporating BH is meant to show a classical general relativity picture, and sort out a few of the issues that may have arisen from the interpretation of physical scenarios based on incorrect diagrams. We purposefully did not try to solve the information paradox, but we learned some things along the way. In similar fashion, we came upon the concept of an evaporating wormhole, and regardless of how such a picture might integrate into our universe, it gives us an interesting mathematical and thought experiment that we hope provides us with more insight into BHs, information, and the limits of analyzing metrics, especially diagramatically.

8.1 What We Did

We developed a methodology of how to model Hawking radiation in a manner that could be plotted by a computer program and therefore, as accurately as our assumptions allow, depict complex and evolving spacetimes. We applied this method and plotting to the formation and evaporation of a BH, and as presented in this thesis, the evaporation of a wormhole.

The methods for explicit computation developed by Schindler [64] and the matching techniques laid out in our paper [65] bring new insight to the open questions surrounding BH evaporation and information preservation. Whether or

not this results in any clarity or a solution to the information paradox actually being accepted is up to the community working on this topic. We certainly hope that the methods and code for computing diagrams will be used widely, as it would be nice to see accurate diagrams in papers rather than sketches (we are a little guilty here of that as well). Physical interpretations of diagrams make much more sense when the diagrams are correct, and perhaps this process also illustrates the limits of using diagrams to interpret and predict the physical world. Certainly in looking at evaporating wormholes we would not so easily have been sure of our conclusions on traversability had we not had computer diagrams to check them.

Our mathematical experiment looking at what happens when an extended Schwarzschild BH (an ER bridge) evaporates involved using junction conditions and energy conservation to determine what matchings are possible. This has shown us that signals could in fact escape a wormhole if it is traversable. Evaporating a wormhole also showed us that an ER bridge can evaporate to a remnant wormhole described by the Ellis metric. We also learned that these objects are inherently different than stellar collapse BHs and this difference is potentially (but likely infeasibly) observable. At the end of it we found a lot of questions and directions in which to continue this work, some of which are foundational.

8.2 Why It Matters

It is a profound experience to explore the physical reality we observe, the interactions between fundamental laws, and delve into the relationship between the mathematics we have come to see as a language to decode our universe. From a more practical and less philosophical perspective, the development of tools to approach problems matters. We explored merely a couple examples of what can be done with matching and explicit computation of Penrose diagrams. But the tools are now there for others to use, and through our couple of explorations we came upon questions that pertain to the fundamental meaning of spacetimes.

From a more practical research standpoint, looking at the evaporation of wormholes is relevant to the current trajectory of research. We see the conversations about reducing wormholes to remnants and wormholes becoming traversable come in towards the discussions of formation mechanisms of wormholes. So here we had a look at both of those ideas simultaneously, and hopefully opened some doors and provoked thought (minimally, our own).

Learning about wormholes now seems like it could be part of reality, and no longer simply another theoretical postulation with no real world backing. Working on this topic and considering that there is a faint chance of it reflecting reality in our universe has been beyond exciting, even if any hope of observation is still long out of range.

Appendix A

Non-Null Junctions

Junction Conditions

Here is a description of the metric junction conditions along non-null hypersurfaces and an example using Schwarzschild and deSitter as well as Schwarzschild and anti-deSitter. This was part of early work on the interior structure of BHs and evaporation matching.

Equations

The metric junction conditions are defined as derived by Israel and using the formalism of Poisson in *A Relativist's Toolkit*[45, 59]. An oversimplified version is presented here. We look at junctions between metrics at an hypersurface, Σ,

which is defined by the function

$$\Phi(x^\alpha) = 0. \tag{A.1}$$

For example, an hypersurface of constant $r, (r = R)$ would have $\Phi = r - R$ (or $\Phi = R - r$, the sign difference of which does not matter). Here general metric coordinates are denoted as x^α and coordinates on the hypersurface are y^a. Note that they are parametric

$$x^\alpha = x^\alpha(y^a), \tag{A.2}$$

and so we can relate the coordinates though

$$e^\alpha_a = \frac{\partial x^\alpha}{\partial y^a}, \tag{A.3}$$

which lie tangent to curves on the hypersurface.

The two junction conditions are

$$\begin{aligned} &1)[h_{ab}] = 0 \\ &2)[K_{ab}] = 0, \end{aligned} \tag{A.4}$$

where h_{ab} is the induced metric on the hypersurface, and K_{ab} is its extrinsic curvature. The brackets indicate the difference $[A] = A^+ - A^-$, and therefore represents a discontinuity in A across the hypersurface. The $-$ superscript indicates the "outside" of the hypersurface, the $+$ the "inside." For ease I will give the main definitions here that I used. The induced metric and extrinsic curvature

are defined as

$$h_{ab} = g_{\alpha\beta} e^{\alpha}_{a} e^{\beta}_{b}, \tag{A.5}$$

and

$$K_{ab} = \nabla_{\beta} n_{\alpha} e^{\alpha}_{a} e^{\beta}_{b}, \tag{A.6}$$

which are composed of the original metrics, the covariant derivative of the normal, and the parametric coordinate vectors. Useful also is the scalar $K \equiv h^{ab} K_{ab} = \nabla_{\alpha} n_{\alpha}$. The ϵ comes from the normals

$$n^{\alpha} n_{\alpha} = \epsilon = \mp 1, \tag{A.7}$$

which will be $-$ for timelike and $+$ for spacelike normals, which means $-$ for spacelike and $+$ for timelike Σ, due to the orthogonality. The normals are defined from the hypersurface function as

$$n_{\alpha} = \frac{\epsilon \partial_{\alpha} \Phi}{\left| g^{\mu\nu} \partial_{\mu} \Phi \partial_{\nu} \Phi \right|^{1/2}}. \tag{A.8}$$

Simplified and written with the brackets for the difference between the outer and inner sides of the hypersurface we have

$$[K_{ab}] = \frac{\epsilon^2}{2} [\partial_{\gamma} g_{\alpha\beta}] n^{\gamma} e^{\alpha}_{a} e^{\beta}_{b} \tag{A.9}$$

for the extrinsic curvature which we can now calculate to determine the junction conditions for particular metrics.

Schwarzschild deSitter

The line elements for the general metrics are:

$$\begin{aligned} \text{Schwarzschild:} \quad ds^2 &= -\left(1-\frac{2M}{r}\right)dt^2 + \left(1-\frac{2M}{r}\right)^{-1}dr^2 + r^2 d\Omega^2 \\ \text{deSitter:} \quad ds^2 &= -\left(1-\frac{r^2}{\alpha^2}\right)dt^2 + \left(1-\frac{r^2}{\alpha^2}\right)^{-1}dr^2 + r^2 d\Omega^2 \end{aligned} \tag{A.10}$$

where $\alpha = \sqrt{\frac{3}{\Lambda}}$ and M is the mass in Schwarzschild. Choosing the hypersurface at a fixed R, we have $y^a = (t, \theta, \phi)$ and $\Phi = R - r$. This gives the induced hypersurface metric line elements as

$$\begin{aligned} \text{Schwarzschild:} \quad dS_+^2 &= -\left(1-\frac{2M}{R}\right)dt^2 + R^2 d\Omega^2 \\ \text{deSitter:} \quad dS_-^2 &= -\left(1-\frac{R^2}{\alpha^2}\right)dt^2 + R^2 d\Omega^2. \end{aligned} \tag{A.11}$$

The first junction condition($[h_{ab}] = 0$) then gives

$$\frac{R^2}{\alpha^2} = \frac{2M}{R}. \tag{A.12}$$

Now onto the second condition. First we have to calculate the normals, and in this case there is just one non-zero component. $\epsilon = -1$ for this spacelike hypersurface.

$$n_-^r = \left(\frac{R^2}{\alpha^2} - 1\right)^{1/2} \quad \text{and} \quad n_+^r = \left(\frac{2M}{R} - 1\right)^{1/2} \tag{A.13}$$

when $R < 2M$ and $\alpha < R$. With this we can get the differences in the extrinsic curvature

$$[K_{tt}] = \frac{1}{2}\left(\frac{-2M}{R^2}\left(\frac{2M}{R} - 1\right)^{1/2} - \frac{2R}{\alpha^2}\left(\frac{R^2}{\alpha^2} - 1\right)^{1/2}\right) \tag{A.14}$$

simplified with the first junction condition this becomes

$$[K_{tt}] = \left(\frac{-3M}{R^2}\right)\left(\frac{2M}{R} - 1\right)^{1/2} \tag{A.15}$$

and

$$[K_{\theta\theta}] = [K_{\phi\phi}] = \frac{1}{2}\left(2R\left(\frac{2M}{R}-1\right)^{1/2} - 2R\left(\frac{R^2}{\alpha^2}-1\right)^{1/2}\right) = 0 \quad \text{by junction condition 1.} \tag{A.16}$$

Since we have a non-zero element left we must calculate the EM tensor at the hypersurface

$$S_{ab} = \frac{-\epsilon}{8\pi}([K_{ab}] - [K]h_{ab}) \tag{A.17}$$

The S_{tt} component goes to zero and we are left only with the angular components

$$S_{\theta\theta} = S_{\phi\phi} = -[K_{tt}]\frac{1}{8\pi} = \frac{3M}{8\pi R^2}\left(\frac{2M}{R} - 1\right)^{1/2} \tag{A.18}$$

which is greater than 0 for $R < 2M$ which is the regime for which this calculation is valid.

The matching of Scwarzschild to anti-deSitter doesn't work because of the sign of the constants.

Appendix B

Overview of Tunneling Picture of Hawking Radiation

In order to justify the use of energy shells as a mechanism for Hawking radiation in the Penrose diagram of an evaporating black hole, there must be a consistent and accepted description of Hawking radiation that allows for this. Following the work of Kraus and Wilczek and Parikh and Wilczek as well as doing analysis of the details of the WKB approximation in this context, one can conclude that looking at Hawking Radiation as tunneling (a particle tunneling description dependent on a non-static background) can be used to join the particle pair picture of Hawking radiation with that of energy shells using the WKB approximation, with reasonable assumptions [50, 58]. In this summary there is a

quick review of the Hamiltonian formalism in general relativity which is used to get the Hamiltonian needed for the tunneling calculation, connections with the path integral action form of the WKB approximation, an overview the Parikh and Wilczek calculation and its justifications, the specifics of allowed particle pair kinematics at a black hole horizon, and how these ideas can be used in the context of Penrose diagrams of black hole evaporation, as well as a discussion about interpretation of this formalism. This section is large derived from and a discussion of the work of Kraus, Parikh, and Wilczek [50, 58], whether it is noted or not below.

It is important to note that though the WKB picture is widely used, so it is good to ensure our matching formalism works with it, it is not the only formulation of Hawking radiation, and our final work of a diagram of an evaporating BH models its shells on the stress-energy tensor flux as it works with Fulling-Davies-Unruh radiation [31, 20, 73]. We do not particularly think that treating evaporation of particles is appropriate but it is nice to make sure the results of multiple formalisms match. This description and discussions is an except from writings prepared but not published on creating a formalism for modeling an evaporating BH.

Hamiltonian Formalism

The derivation of the Hamiltonian of the changing black hole in Kraus and Wilczek follows general ADM formalism methodology as is used by Aguirre and Johnson and Fischler, Morgan, and Polchinski [50, 30, 47]. The formalism used in the

tunneling picture is best understood through a combination of the Hamiltonian formalism of GR and the path integral formalism of the WKB approximation which will be covered in the next section. The goal of Kraus and Wilczek is to determine a way to incorporate the self-gravitation of the outgoing matter and thus include a non-static background, something that is missing from the original formulation. Parikh and Wilczek continue down this path to actually calculate the Hawking temperature from the action in this self-gravitating scenario [58].

In the ADM formalism one begins by writing the metric line element in the form

$$ds^2 = -N^t(t,r)^2 dt^2 + L(t,r)^2[dr + N^r(t,r)dt]^2 + R(t,r)^2(d\theta^2 + \sin^2\theta d\phi^2) \quad \text{(B.1)}$$

where N^t is the lapse and N^r is the shift, $L \equiv \frac{ds}{dr}$, and R is the transverse radius. We will be looking at a spherically symmetric case. Through the metric you have the action in canonical form, a coupled combination of gravity and a general matter theory

$$S = \int dt\, p\, \dot{q} + \int dr dt\, (\pi_L \dot{L} + \pi_R \dot{R} - N^t H_t - N^r H_r) \quad \text{(B.2)}$$

where π_L and π_R are the conjugate momenta and H_t and H_r and the components of the hamiltonian. In the case of Kraus and Wilczek they are looking for the action of a shell, so they separate the hamiltonian into a spherical shell part and the overall gravitational part, the action of the shell coming from

$$S^s = -m \int \sqrt{-\hat{g}_{\mu\nu} d\hat{x}^\mu d\hat{x}^\nu} = -m \int dt \sqrt{(\hat{N}^t)^2 - \hat{L}^2(\dot{\hat{r}} + \hat{N}^r)^2} \quad \text{(B.3)}$$

with m being the rest mass of the shell and the hats indicating that the terms are to be evaluated on the shell. This results in the full action for the shell and the gravity system of

$$S = \int dt\, p\, \dot{\hat{r}} + \int dr dt\, (\pi_L \dot{L} + \pi_R \dot{R} - N^t(H_t^s + H_t^G) - N^r(H_r^s + H_r^G) - \int dt\, M_{ADM} \tag{B.4}$$

where the $\hat{r}$ in the first term is to be evaluated for the shell, and the last term has M_{ADM} which is the ADM mass. They then do an incredible amount of algebra using the ADM formalism (finding conjugate momenta, defining shell mass discontinuity etc.) that has been looked though, but which will not be repeated here, to find an effective action for only the shell (and included is the hamiltonian). So finally they get the canonical action

$$S = \int dt\, [p_c \dot{\hat{r}} - M_+] \tag{B.5}$$

where p_c is the canonical momentum and thus M_+ is the hamiltonian. They had previously defined M_+ as the mass when $r > \hat{r}$ and M as the mass when $r < \hat{r}$. They note that this is only the hamiltonian or a restricted set of gauges, details of this can be determined by looking at the conjugate momenta.

Now this is quantized and turned into a useable effective action, so the particle contribution is pulled out of the particle contribution to the hamiltonian with

$$M_+ = M - p_t \tag{B.6}$$

where p_t is the temporal part of the momentum, and the action looks like

$$S = \int dt \, [p_c \dot{\hat{r}} + p_t] \tag{B.7}$$

as the overall M term is dropped as it only contributes a constant. Finally we have a form to use in the WKB approximation

$$S = \int [p\dot{r} + p_t] \tag{B.8}$$

$$p = \pm\sqrt{p_t^2 - m^2} \tag{B.9}$$

where m is the mass of the shell/particle, and r now directly refers to the shell.

WKB

The WKB approximation is best described for this case with the action through the path integral. Given the above action Parikh and Wilczek set forth the following arguments as to why a particle tunneling WKB approximation is justifiable. It is undeniably important that changing background geometry is taken into account, and that energy conservation actually gets enforced. They state that using dynamical geometry means that you can get energy conservation [58]

Parikh and Wilczek use Painlevé coordinates, which are one example of coordinates that are non-singular at the horizon

$$t = t_s + 2\sqrt{2Mr} + 2M \ln\left(\frac{\sqrt{r} - \sqrt{2M}}{\sqrt{r} + \sqrt{2M}}\right) \tag{B.10}$$

where t_s is the Schwarzschild time. This changes the Schwarzschild metric line element to

$$ds^2 = -\left(1 - \frac{2M}{r}\right) dt^2 + 2\sqrt{\frac{2M}{r}}\, dtdr = dr^2 + r^2 d\Omega^2. \tag{B.11}$$

Now this has radial null geodesics

$$\dot{r} = \pm 1 - \sqrt{\frac{2M}{r}}, \tag{B.12}$$

with the sign depending on whether they are outgoing (+) or ingoing (-). Following the work in Kraus and Wilczek, the metric changes when we consider self-gravitating shells. Using a fixed black hole mass and a changing ADM mass the shells will travel along geodesics now given by

$$ds^2 = -\left(1 - \frac{2(M-\omega)}{r}\right) dt^2 + 2\sqrt{\frac{2(M-\omega)}{r}}\, dtdr = dr^2 + r^2 d\Omega^2, \tag{B.13}$$

where ω is the mass/energy content of the shell. The hamiltonian is now $M - \omega$ and the geodesics will take the form above with $M \to M - \omega$.

Now we can perform the WKB approximation for tunneling. Parikh and Wilczek say we may approximate the shell as a point particle, thus allowing WKB, because the outgoing wave will be blue-shifted for an observer near the horizon and the radial wave number will go to infinity. The action we are calculating is for the shell, now a particle. We look at an S-wave, outgoing particle with positive energy that crosses the horizon from r_{in} to r_{out}, keeping in mind that $r_{in} > r_{out}$.

The imaginary part of the action is taken here because it represents the unstable energy states, which are the ones that will tunnel [18]. The action is

$$\mathrm{Im}S = \mathrm{Im}\int_{r_{in}}^{r_{out}} p_r\, dr = \mathrm{Im}\int_{r_{in}}^{r_{out}}\int_0^{p_r} dp_r\, dr \tag{B.14}$$

where in the second term we turn the momentum into a full integral as well. Next a few substitutions; using the hamiltonian form we have

$$\dot{r} = +\frac{dH}{dp_r}\bigg|_r, \tag{B.15}$$

this is used to substitute p_r and the units on the integral must also change from momentum to energy (from the hamiltonian). This gives the first term in

$$\mathrm{Im}S = \mathrm{Im}\int_M^{M-\omega}\int_{r_{in}}^{r_{out}} \frac{dr}{\dot{r}} dH = \mathrm{Im}\int_0^{\omega}\int_{r_{in}}^{r_{out}} \frac{dr}{1-\sqrt{\frac{2(M-\omega')}{r}}}(-d\omega'), \tag{B.16}$$

the second term comes from substituting in the geodesic form of $\dot{r}$ and adding in the definition of $H = M - \omega$ and seeing that dH only changes due to ω as M is constant. This integral is now evaluated by contour, so that the positive energy solutions decay in time (this corresponds to the lower half plane in ω'). This results in

$$\mathrm{Im}S = +4\pi\omega\left(M - \frac{\omega}{2}\right) \tag{B.17}$$

where to get this we also must have $r_{in} = 2M$ and $r_{out} = 2(M-\omega)$. This gives us the initial and final positions of the particle; starting at $2M - \epsilon$ and going to $2(M-\omega) + \epsilon$.

By definition then the semi-classical tunneling rate is

$$\Gamma \sim e^{-2\mathrm{Im}S} = e^{-8\pi\omega\left(M-\frac{\omega}{2}\right)} = e^{+\Delta S_{B-H}}, \tag{B.18}$$

where ΔS_{B-H} is the change in the Bekenstein-Hawking entropy. Note that the rate is not exact because it requires a pre-factor, but the important information lies in the exponent. They ignore the quadratic term in the exponent and say that this result is composed of a Boltzmann factor and a Hawking temperature of $\frac{1}{8\pi M}$. The spectral flux will have the form

$$\rho(\omega) = \frac{d\omega}{2\pi}\frac{\left|T(\omega)\right|^2}{e^{+8\pi M\omega}-1} \tag{B.19}$$

with $\left|T(\omega)\right|^2$ being the greybody transmission coefficient.

This WKB approximation deviates from what is usually done because here the background itself changes. We had found examples of a classical analogue have been found for this thus far, but it is figured that a careful treatment of atomic decay with a changing electromagnetic potential should be similar.

Parikh and Wilczek show briefly that their WKB integrals end up exactly the same for an antiparticle or "negative" energy particle tunneling in. Because it travels back in time they reverse the sign in the equations of motion. This, they say, would mean an extra factor of two would have to turn up in the pre-factor, but will not affect the exponent and thus not the temperature result either.

Though here the final and initial positions of the tunneling particle would have to be $2(M+\omega)+\epsilon$ initially and $2M-\epsilon$ finally. The assumed pair creations would end up looking very different. The matter particles that end up outside the black hole would have different positions given whether particle or antiparticle tunneling took place. Even if the path integrals for the particle inside and antiparticle outside tunneling are the same, the assumed pair creation scenarios associated with them are different and pictorial representations struggle to make them look alike.

Particle Kinematics

The WKB approximation above can be interpreted to be part of some sort of particle kinematics scenario at the horizon. Parikh and Wilczek give one version of this but it is not entirely clear that this interpretation is complete or that there are not other ways to look at it. Their statements directly say that the tunneling path integral represents a particle or antiparticle, created by vacuum particle pair created just inside or just outside the horizon. If inside the matter particle tunnels out, if outside the antimatter particle tunnels in.

The figures here are possible pictures based on the Parikh and Wilczek and final radial values. Figure B.1 shows the arrow and line colors and styles that represent different aspects of the tunneling picture in the diagrams. In figure B.2 pair creation inside horizon and outside are shown, along with possible tunneling mechanics. Figure B.3 shows another possibility of what the antiparticle tunneling

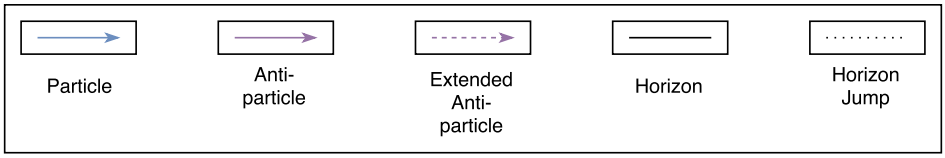

Figure B.1: Key of notation in the following diagrams.

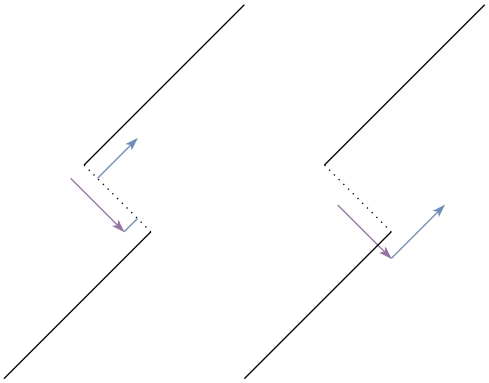

Figure B.2: Pair creation and tunneling inside the horizon on the left, pair creation outside on the right.

version is trying to describe. It is not clear what this really means or if it makes physical sense; there is necessity here for a discussion of what constitutes an antiparticle.

There are other possibilities for where the particles came from and what processes could allow for particles to exist near enough to the horizon to tunnel. Figure B.4 demonstrates that what can appear to be the antiparticle could be space-like tunneling or otherwise, thus we show an extended antiparticle coming from farther in. If for instance the particle came from inside the black hole by way of some other tunneling or path it could appear to be as in figure B.5, where

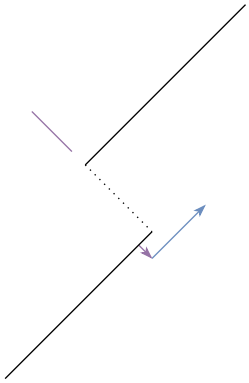

Figure B.3: One possibility of what the exterior pair creation is supposed to mean.

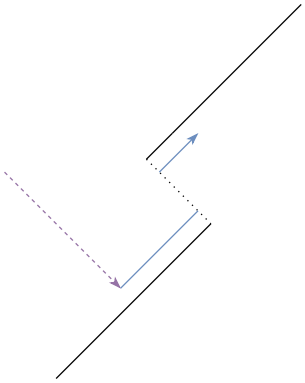

Figure B.4: Pair creation inside the horizon, with extended particles.

the particles originates inside and then tunnels, appearing to be an antiparticle before tunneling again to exit as described the the WKB above. The mathematics and allowance of this trajectory still needs to be looked into.

Though it was mentioned at the end of the WKB description it is important to note that the final results of the tunneling pictures would result in different locations of the particle outside. Compare, for instance, the left and right sides of figure B.2 and one can see that in the final state the particle is at $2(M-\omega)+\epsilon$

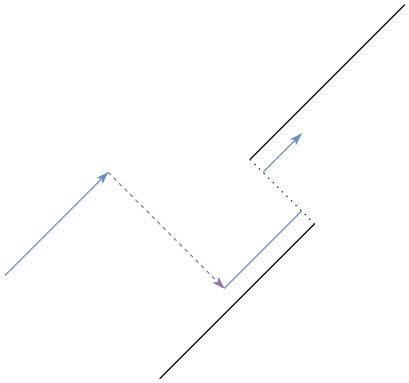

Figure B.5: Apparent pair creation with alternate anti-particle genesis.

on the left and $2(M+\omega)+\epsilon$ on the right.

Given these scenarios and an identical path integral, our interpretation now depends somewhat which we take to be more fundamental. Parikh and Wilczek state that you must have two identical contributions and the doubling factor will go in the pre-factor that is rarely calculated, complex, and dependent on frequency. It is relevant to some extent though if you want to interpret what exactly is happening. Conversely to Parikh and Wilczek's argument one might be able to say that if the path is the same, and they are indistinguishable processes, that one integral would account for both because perhaps vacuum pair creation is not the root of the existence of the tunneling matter in the first place. It is important to note here too that this process would not particularly be observable, and when integrating the particle picture into a classical diagram in general relativity one has to figure the process is hidden by some quantum screen. The particle and

shell assumptions are enough to allow the math to work.

Discussion

General use of tunneling in our Penrose diagram work:

Given that this approximation works, and is well accepted (many, many citations, most of which use the formulation, a few of which calculate further, and a couple of which disagree), and is consistent in both the energy shell, and via connection though WKB approximation the particle pair picture, it should be fine to use energy shells to represent the tunneling as the evaporation part of the picture in a Penrose diagram.

There are some things to keep in mind and a few outstanding issues left. The confusing nature of the pre-factor and the particle picture is one issue. What do multiple identical paths in the path integral mean? Are we or are we not really summing Feynman diagrams? If you have identical integrals it doesn't matter so much that it can match a pair formation picture, though it works for it, but that more importantly the integral describes one picture of matter escape. This can probably be interpreted and used rather than trying to describe a particular particle mechanism. No concrete conclusions have been reached about this, but it seems possible to move on without it since the doubling factor would turn up in the pre-factor anyway. Most follow-up work wants to account for the temporal part of the action and quantum corrections to the temperature.

It is also important to remember to note that the particle diagrams are not correct Penrose diagrams and should be thought of as hiding behind quantum shields. Especially given that this formalism of the particle WKB makes the result be in the form a spherical shells (again allowable because of the approximations used).

Vaidya could probably be applied here to represent the shells, but not clear if that's the best thing to do and not simply layers or lower mass Schwarzschild. One would have to verify that the energy-momentum tensor matches. The Vaidya one has been verified a couple of times. Some discussion of sign might be necessary.

Other thoughts and continuation:

Especially if we would like to use the tunneling calculation to describe the end of a different method of matter escape instead of pair creation it would be important to compare other methods of deriving Hawking radiation. Also, if following the possibility of space-like tunneling, we also need to investigate the relationship between null and non-null versions and what is allowable by energy conditions and so forth.

The whole tunneling calculation is not dependent on pair creation. It simply gives us the probability of a particle getting from r_{in} to r_{out} with that being outside the new horizon.

There was a discussion originally about how to understand what happens

to momentum and energy conservation as a particle crosses the horizon, and whether there is anything to take into account for the apparent trajectories of the particle due to changes in the metric (switching of time and space coordinates). We decided the particle cannot see anything unusual at horizon, so its vector must be able to be parallel transported about. In the tunneling calculation the Painlevé coordinates should account for this. We moved on from any discussion necessitating linking to Killing vectors, such as in Hartle, because that is not commonly thought of that way anymore. The tunneling movement is sensible because the particle moves inward and thus conserves energy. Other attempts to enforce some sort of conservation where the particle components change can only mean something to an observer. In the right coordinates the particle trajectories can maintain direction and parallel transport without worry or non-conservation.

Final thoughts

The tunneling formalism is very interesting, but likely not the best way to look at Hawking radiation, especially for a Penrose diagram picture where we can use flux shells based on the stress energy tensor. It does describe the process of a particle tunneling out of a black hole at the horizon, regardless of why it is there to do so, which may be interesting in its own right. Lastly the way the WKB approximation takes into account the changing background is a good exposition of the complexity of a process changing background assumptions and the importance

in these pictures to keep good track of such things.

Bibliography

[1] M. Ackermann et al. Search for Gamma-Ray Emission from Local Primordial Black Holes with the Fermi Large Area Telescope. *Astrophys. J.*, 857(1):49, 2018.

[2] Anthony Aguirre and Matthew C. Johnson. Two tunnels to inflation. *Phys. Rev.*, D73:123529, 2006.

[3] S. Alexander, R. Brandenberger, and D. Easson. Brane gases in the early Universe. *Phys. Rev. D*, 62(10):103509, Nov 2000.

[4] Ahmed Almheiri, Donald Marolf, Joseph Polchinski, and James Sully. Black Holes: Complementarity or Firewalls? *JHEP*, 02:062, 2013.

[5] Dongsu Bak, Chanju Kim, and Sang-Heon Yi. Transparentizing Black Holes to Eternal Traversable Wormholes. *JHEP*, 03:155, 2019.

[6] C. Barrabes and P. A. Hogan. Detection of impulsive light - like signals in general relativity. *Int. J. Mod. Phys.*, D10:711–722, 2001.

[7] C. Barrabès and W. Israel. Thin shells in general relativity and cosmology: The lightlike limit. *Phys. Rev. D*, 43:1129–1142, Feb 1991.

[8] Daniel Barraco and Victor H. Hamity. Maximum mass of a spherically symmetric isotropic star. *Phys. Rev. D*, 65:124028, Jun 2002.

[9] Anshuman Baruah and Atri Deshamukhya. Traversable Wormholes in Higher Dimensional Theories of Gravity. 2019.

[10] Jacob D. Bekenstein. Black holes and entropy. *Phys. Rev. D*, 7:2333–2346, Apr 1973.

[11] Jacob D. Bekenstein. Generalized second law of thermodynamics in black-hole physics. *Phys. Rev. D*, 9:3292–3300, Jun 1974.

[12] Eric Blackman. Giants of physics found white-dwarf mass limits. *Nature*, 440(7081):148, Mar 2006.

[13] K.A. Bronnikov and V.G. Krechet. Potentially observable cylindrical wormholes without exotic matter in general relativity. *Phys. Rev.*, D99(8):084051, 2019.

[14] M. Brooks. *The Big Questions: Physics*. Big questions. Quercus, 2013.

[15] Ral Carballo-Rubio, Francesco Di Filippo, Stefano Liberati, Costantino Pa-

cilio, and Matt Visser. On the viability of regular black holes. *JHEP*, 07:023, 2018.

[16] Bernard J. Carr. Primordial black holes: Recent developments. *eConf*, C041213:0204, 2004.

[17] Sean M. Carroll. *Spacetime and geometry: An introduction to general relativity*. 2004.

[18] S. Coleman. *Aspects of Symmetry: Selected Erice Lectures*. Cambridge University Press, 1988.

[19] Sidney Coleman and Frank De Luccia. Gravitational effects on and of vacuum decay. *Phys. Rev. D*, 21:3305–3315, Jun 1980.

[20] P. C. W. Davies. Scalar production in Schwarzschild and Rindler metrics. *Journal of Physics A Mathematical General*, 8(4):609–616, Apr 1975.

[21] P. C. W. Davies, S. A. Fulling, and W. G. Unruh. Energy Momentum Tensor Near an Evaporating Black Hole. *Phys. Rev.*, D13:2720–2723, 1976.

[22] Ujjal Debnath, Mubasher Jamil, Ratbay Myrzakulov, and M. Akbar. Thermodynamics of Evolving Lorentzian Wormhole at Apparent and Event Horizons. *International Journal of Theoretical Physics*, 53(12):4083–4094, Dec 2014.

[23] Heling Deng, Jaume Garriga, and Alexander Vilenkin. Primordial black hole and wormhole formation by domain walls. *JCAP*, 1704(04):050, 2017.

[24] Heling Deng and Alexander Vilenkin. Primordial black hole formation by vacuum bubbles. *JCAP*, 1712(12):044, 2017.

[25] P. A. M. Dirac. The Quantum Theory of the Electron. *Proceedings of the Royal Society of London Series A*, 117(778):610–624, Feb 1928.

[26] Tevian Dray and Gerard 't Hooft. The effect of spherical shells of matter on the schwarzschild black hole. *Comm. Math. Phys.*, 99(4):613–625, 1985.

[27] A. Einstein and N. Rosen. The particle problem in the general theory of relativity. *Phys. Rev.*, 48:73–77, Jul 1935.

[28] H. G. Ellis. Ether flow through a drainhole: A particle model in general relativity. *Journal of Mathematical Physics*, 14:104–118, January 1973.

[29] Edward Farhi and Alan H. Guth. An obstacle to creating a universe in the laboratory. *Physics Letters B*, 183(2):149–155, Jan 1987.

[30] W. Fischler, D. Morgan, and J. Polchinski. Quantization of false-vacuum bubbles: A hamiltonian treatment of gravitational tunneling. *Phys. Rev. D*, 42:4042–4055, Dec 1990.

[31] Stephen A. Fulling. Nonuniqueness of Canonical Field Quantization in Riemannian Space-Time. *Phys. Rev. D*, 7(10):2850–2862, May 1973.

[32] Jaume Garriga, Alexander Vilenkin, and Jun Zhang. Black holes and the multiverse. *JCAP*, 1602(02):064, 2016.

[33] Jonathan Gratus, Paul Kinsler, and Martin W. McCall. Evaporating black-holes, wormholes, and vacuum polarisation: must they always conserve charge? *Found. Phys.*, 49(4):330–350, 2019.

[34] Alan H. Guth. Inflationary universe: A possible solution to the horizon and flatness problems. *Phys Rev D*, 23(2):347–356, Jan 1981.

[35] J.B. Hartle. *Gravity: An Introduction to Einstein's General Relativity*. Addison-Wesley, 2003.

[36] S. W. Hawking. Particle Creation by Black Holes. *Commun. Math. Phys.*, 43:199–220, 1975.

[37] S. W. Hawking and G. F. R. Ellis. *The Large Scale Structure of Space-Time*. Cambridge Monographs on Mathematical Physics. Cambridge University Press, 2011.

[38] Stephen Hawking. Gravitationally collapsed objects of very low mass. *MNRAS*, 152:75, Jan 1971.

[39] Stephen W. Hawking, Malcolm J. Perry, and Andrew Strominger. Soft Hair on Black Holes. *Phys. Rev. Lett.*, 116(23):231301, 2016.

[40] Sean A. Hayward. Black holes and traversible wormholes: A Synthesis. In *Proceedings, 11th Workshop on General Relativity and Gravitation (JGRG11): Tokyo, Japan, January 9-12, 2002*, 2002.

[41] Sean A. Hayward. Formation and evaporation of regular black holes. *Phys. Rev. Lett.*, 96:031103, 2006.

[42] Sean A. Hayward. Wormhole dynamics. In *On recent developments in theoretical and experimental general relativity, astrophysics and relativistic field theories. Proceedings, 12th Marcel Grossmann Meeting on General Relativity, Paris, France, July 12-18, 2009. Vol. 1-3*, pages 1151–1153, 2009.

[43] Sean A. Hayward and Hiroko Koyama. How to make a traversable wormhole from a Schwarzschild black hole. *Phys. Rev.*, D70:101502, 2004.

[44] Gary T. Horowitz, Don Marolf, Jorge E. Santos, and Diandian Wang. Creating a Traversable Wormhole. 2019.

[45] W. Israel. Singular hypersurfaces and thin shells in general relativity. *Il Nuovo Cimento B (1965-1970)*, 44(1):1–14, Jul 1966.

[46] Mubasher Jamil and M. Akbar. Wormhole Thermodynamics at Apparent Horizons. 2009.

[47] Matthew C. Johnson, Carroll L. Wainwright, Anthony Aguirre, and Hiranya V. Peiris. Simulating the Universe(s) III: Observables for the full bubble collision spacetime. *JCAP*, 1607(07):020, 2016.

[48] Maxim Yu. Khlopov. Primordial Black Holes. *Res. Astron. Astrophys.*, 10:495–528, 2010.

[49] Hiroko Koyama and Sean A. Hayward. Construction and enlargement of traversable wormholes from Schwarzschild black holes. *Phys. Rev.*, D70:084001, 2004.

[50] Per Kraus and Frank Wilczek. Selfinteraction correction to black hole radiance. *Nucl. Phys.*, B433:403–420, 1995.

[51] M. D. Kruskal. Maximal extension of schwarzschild metric. *Phys. Rev.*, 119:1743–1745, Sep 1960.

[52] Kimyeong Lee and Erick J. Weinberg. Decay of the true vacuum in curved space-time. *Phys. Rev. D*, 36:1088–1094, Aug 1987.

[53] Juan Maldacena and Leonard Susskind. Cool horizons for entangled black holes. *Fortsch. Phys.*, 61:781–811, 2013.

[54] Donald Marolf. The Black Hole information problem: past, present, and future. *Rept. Prog. Phys.*, 80(9):092001, 2017.

[55] M. S. Morris and K. S. Thorne. Wormholes in space-time and their use for interstellar travel: A tool for teaching general relativity. *Am. J. Phys.*, 56:395–412, 1988.

[56] T. Padmanabhan. *Gravitation: Foundations and Frontiers*. Cambridge University Press, 2010.

[57] Don N. Page. Hawking radiation and black hole thermodynamics. *New J. Phys.*, 7:203, 2005.

[58] Maulik K. Parikh and Frank Wilczek. Hawking radiation as tunneling. *Phys. Rev. Lett.*, 85:5042–5045, 2000.

[59] E. Poisson. *A Relativist's Toolkit: The Mathematics of Black-Hole Mechanics*. Cambridge University Press, 2004.

[60] Eric Poisson. A Reformulation of the Barrabes-Israel null shell formalism. 2002.

[61] Joseph Polchinski. The Black Hole Information Problem. In *Proceedings, Theoretical Advanced Study Institute in Elementary Particle Physics: New Frontiers in Fields and Strings (TASI 2015): Boulder, CO, USA, June 1-26, 2015*, pages 353–397, 2017.

[62] Ian H. Redmount. Blue-Sheet Instability of Schwarzschild Wormholes. *Progress of Theoretical Physics*, 73(6):1401–1426, 06 1985.

[63] Nayan Sarkar, Susmita Sarkar, Farook Rahaman, P. K. F. Kuhfittig, and G. S. Khadekar. Possible formation of wormholes from dark matter in an isothermal galactic halo and void. 2019.

[64] J. C. Schindler and A. Aguirre. Algorithms for the explicit computation of Penrose diagrams. *Class. Quant. Grav.*, 35(10):105019, 2018.

[65] J.C. Schindler, A. Aguirre, and A. Kuttner. Visualizing black hole evaporation with explicitly computed penrose diagrams. In Preparation.

[66] Karl Schwarzschild. On the gravitational field of a mass point according to Einstein's theory. *Sitzungsber. Preuss. Akad. Wiss. Berlin (Math. Phys.)*, 1916:189–196, 1916.

[67] Hisa-aki Shinkai and Sean A. Hayward. Fate of the first traversible wormhole: Black hole collapse or inflationary expansion. *Phys. Rev.*, D66:044005, 2002.

[68] Alex Simpson, Prado Martin-Moruno, and Matt Visser. Vaidya spacetimes, black-bounces, and traversable wormholes. 2019.

[69] Paul J. Steinhardt and Neil Turok. The cyclic model simplified. *New Astronomy Reviews*, 49:43–57, May 2005.

[70] P.J. Steinhardt, V.F. Mukhanov, V. Mukhanov, Cambridge University Press, and M. Viatcheslav. *Physical Foundations of Cosmology*. Cambridge University Press, 2005.

[71] L. Susskind. *The Black Hole War: My Battle with Stephen Hawking to Make the World Safe for Quantum Mechanics*. Little, Brown, 2008.

[72] Leonard Susskind, Larus Thorlacius, and John Uglum. The Stretched horizon and black hole complementarity. *Phys. Rev.*, D48:3743–3761, 1993.

[73] W. G. Unruh. Notes on black-hole evaporation. *Phys. Rev. D*, 14(4):870–892, Aug 1976.

[74] Alexander Vilenkin. Birth of inflationary universes. *Phys Rev D*, 27(12):2848–2855, Jun 1983.

[75] Carroll L. Wainwright, Matthew C. Johnson, Hiranya V. Peiris, Anthony Aguirre, Luis Lehner, and Steven L. Liebling. Simulating the universe(s): from cosmic bubble collisions to cosmological observables with numerical relativity. *JCAP*, 1403:030, 2014.

[76] Robert M. Wald. *General Relativity*. Chicago Univ. Pr., Chicago, USA, 1984.

[77] Ya. B. Zel'dovich and I. D. Novikov. The Hypothesis of Cores Retarded during Expansion and the Hot Cosmological Model. *Astronomicheskii Zhurnal*, 43:758, Jan 1966.